Master's Thesis

Communication-Aware Multi-Target Tracking Guidance for Cooperative UAVs with Gimbaled Vision Sensors in Urban Environments

Jinwoo Oh

Department of Mechanical Engineering
(Mechanical Engineering)

Ulsan National Institute of Science and Technology

2021

Communication-Aware Multi-Target Tracking Guidance for Cooperative UAVs with Gimbaled Vision Sensors in Urban Environments

Jinwoo Oh

Department of Mechanical Engineering

Ulsan National Institute of Science and Technology

Communication-Aware Multi-Target Tracking Guidance for Cooperative UAVs with Gimbaled Vision Sensors in Urban Environments

A thesis/dissertation submitted to
Ulsan National Institute of Science and Technology
in partial fulfillment of the
requirements for the degree of
Master of Science

Jinwoo Oh

12/10/2020 of submission

Approved by
_____
Advisor
Hyondong Oh

Communication-Aware Multi-Target Tracking Guidance for Cooperative UAVs with Gimbaled Vision Sensors in Urban Environments

Jinwoo Oh

This certifies that the thesis/dissertation of Jinwoo Oh is approved.

12/10/2020 of submission
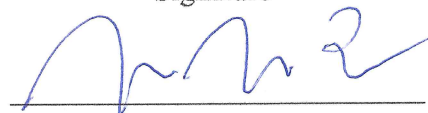
Signature

_____

Advisor: Hyondong Oh

Signature

_____

Cheolhyeon Kwon

Signature

_____

Jeonghwan Jeon

Signature

Abstract

This paper proposes the unified cooperative multi-target tracking algorithm, which considers the sensing range and communication in an urban environment. The objective function of the proposed algorithm is composed of two terms. The first-term is formulated by using FIM. Since Fisher information matrix can be utilized to quantify the information gathered by the sensors, we can formulate an objective function that reflects the constraints like the sensor field of view(FOV). Also, by reflecting parameters related to communication, communication with the ground station can be considered. However, if the target is outside the sensing range or occluded by the building continuously, UAVs cannot capture this target in the prediction step of receding horizon method when the first-term is used only.

To solve this problem, the second-term, which is made up of relative distance between targets and UAVs, is proposed. In this situation, the uncertainty increases because the target information cannot be obtained. As the uncertainty increases, the increasing weight is multiplied by the second-term to generate a path to reduce the distance to this target. If the distance to the target is within the sensing range by using this term, the target can be tracked again by using the first-term because the uncertainty decreases by the sensing.

The main contributions of this thesis are as follows. First, UAVs can create a path and a gimbal command to get useful information by considering the limited sensing capability. Second, by considering communication, the communication stability has been improved and the amount of information in the ground station has been increased. Lastly, in the prediction step of the receding horizon method, the target can be tracked even when information about the target is not gathered.

Contents

List of Figures

I   Introduction

1.1   Background and Motivation

As over the past few decades, as computing power and sensor performance have improved, unmanned aerial vehicles (UAVs) have been used for various applications. Examples of such missions include police patrol [1], search and exploration for rescue [2–4], target tracking [5, 6], and persistent surveillance [7]. Although these missions require different requirements in various environments, they aim to reduce the uncertainty of the information about a target while collecting as much information as possible.

As technology advances, these ISR processes are being carried out using UAVs. In particular, a small UAV equipped with a gimbal vision sensor and communication module can cover a wide area with a small number of UAVs for these applications. Especially, interesting ISR missions using multiple small UAV are target states estimation and tracking. Pixel coordinates for targets obtained from the vision sensor, combined with position and attitude from UAV, can be used to estimate the state of the target, which can be used to track the target persistently [8]. Various studies have been conducted for a target tracking mission autonomously [9–13]. However, even if performing the autonomous mission, we need to consider the communication between UAVs and the ground station to judge if the mission is failed or plan the next mission based on UAVs' information.

Two technical issues arise when multiple UAVs track multiple targets in a cooperative target tracking mission considering communication with ground stations: (1) target state estimation and (2) path planning.; In order to reduce the estimation error and the uncertainty of the estimate, it is necessary to improve the performance of the estimator itself or to develop an efficient method for fusing the target information obtained from multiple UAVs. Path planning; It covers how to create a path to achieve specific goals such as maximizing information about the target, persistent tracking, and maintaining communication.

In this work, we use the information form of the Extended Kalman filter to fuse the information for target gathered by multiple UAVs. The planning algorithm is also proposed to achieve a certain objective using receding horizon method considering various constraints.

1.2   Related Work

Target state estimation is one of the most important studies in the target tracking field. In the target tracking application, the sensor of the UAV can acquire measurements like a range or bearing angle to the UAV's position. Kalman filter, which uses this type of measurement, is developed in variety. In a cooperative mission, each UAV can communicate with each other and exchange information about the target through the communication module. Information filter is a common estimation method, which is another form of Kalman filter [14]. In the case of IF, the information vector and information matrix are used for estimation instead of the

state vector and covariance matrix. Also, since the measurement is reflected in the information matrix, it has the advantage of being fused by simply adding the information matrix [15, 16]. For this reason, the information filter is widely used in data fusion problems using multi-sensors. Not only this, various algorithms based on information filters have been developed. Ridley [17] proposed a decentralized aerial data fusion system based on information filter to track multiple ground moving target. He also covered hardware and software issues that may arise when operating these systems. Casbeer [18] proposed a distributed information filtering method using a consensus filter. The information consensus filter proposed in this work is a distributed filter, and each UAV maintains a local estimation filter, but the consensus filter is responsible for communication with neighbors. Kim [19] proposed an unscented information filter. To deal with the nonlinear system, the linearization error is mitigated through the unscented transformation. Through these studies, it is confirmed that information could effectively fuse measurements obtained from multiple UAVs.

Path planning is another important area that is covered in this study. This issue focuses on generating trajectories to achieve a certain objective. Various earlier research has developed UAV path planning methods, including the gradient-based control law, standoff tracking, and receding horizon optimization (RHO).

In the gradient-based method, in order to minimize the determinant or trace of the error covariance matrix in each sensor platform, the gradient of a specific metric is calculated and optimized using this. Yang [20] calculated the gradient of the determinant of the covariance matrix in order to maximize the expected information from its sensor and then performed path planning using this. Chung [21] proposed a method to minimize the cost function by using a gradient-descent-based manner to reduce sensing uncertainty. Similarly, Schlotfeldt [22] considered the problem of reducing the estimation uncertainty of the team of robots. However, these methods have the disadvantage that they can be easily trapped in local optima and kinematics constraints are not considered.

Earlier studies using various methods have been conducted to perform standoff tracking. First, a standoff tracking method using vector field is proposed [23–25]. Shin [23] proposed a nonlinear disturbance observer-based standoff tracking method. Disturbances such as wind and model uncertainty are compensated through a nonlinear disturbance observer. Chen [24] provided target tracking and obstacle avoidance algorithm by combining Lyapunov vector field guidance and tangent vector field guidance. Lim [25] proposed a modified vector field for multiple UAVs that can consider various constraints. Park [26] proposed a standoff tracking algorithm using the sidebearing angle. To obtain the sidebearing angle, the pixel coordinate in the image plane and the state of the UAV are used. Wu [26] provided a standoff tracking guidance law based on a sliding mode control. The finite-time convergence and robustness of the proposed algorithm are verified using Lyapunov theory.

Finally, various planning techniques using the receding horizon method are proposed. Receding horizon control, also called Model predictive control (MPC), is a technique that creates

2

a control action considering various constraints such as the dynamics of the UAV, information about the environment, and future costs during the time to predict. Peng [27] proposed the MPC-based target tracking algorithm that considers various constraints such as sensor coverage and obstacles in urban environments. In order to solve the optimization problem, an improved gray wolf optimizer(IGWO) were used. This algorithm generates both 2D and 3D paths are generated. Sharma [28] developed a cooperative sensor resource management (CSRM) technique to geolocate multiple ground moving targets using a group of fixed-wing UAVs. An MPC-based unified algorithm that generates the trajectory of the UAVs and the gimbal direction command mounted on the UAV is proposed. Farmani [29] performed a similar study to [28], but the planning is carried out by separating the path and gimbal direction. [28] and [29] deal with the cooperative target tracking problem but do not consider the urban environment and communication. Skoglar [30] proposed a target search and tracking algorithm considering FOV in an urban environment. The search and tracking modes are switched according to the estimation uncertainty, and at this time, an appropriate single UAV trajectory and gimbal direction command are generated. Liu [31] proposed an algorithm for cooperative target tracking while considering communication with the ground station. However, there is a limitation that the urban environment and multi-target are not considered.

From these various previous studies, it can be seen that a unified cooperative multi-target tracking algorithm is needed, which considers the urban environment, communication, and sensing range. This paper proposes a unified algorithm that generates trajectory and gimbal direction commands while maintaining communication between the ground station and UAV and gathering useful information about the target.

1.3   Contribution of the Thesis

Based on the contents of the previous section, this thesis paper proposes the information-theoretic receding horizon based algorithm that plans desired roll input and gimbal direction input for UAVs. The main contributions of this thesis are as follows.

First, UAVs can create a path and a gimbal command to get useful information by considering the limited sensing capability. The constraints may include the sensing range, camera FOV, and occlusion by the buildings.

Second, by considering communication, the probability of the successful transmission between the ground station and UAVs has been improved. As a result, the amount of information from the ground station and the stability of communication between the ground station and UAVs have increased, allowing the human operator at the ground station to understand the overall situation.

Lastly, even when information cannot be obtained from any input in the prediction process of the receding horizon method due to various constraints, the target can be continuously tracked through the proposed algorithm. Unlike previous works that use the objective function formalized using only the scalar metric of Fisher information matrix, the success rate of the

cooperative multi-target tracking mission is improved by an additional objective function that can consider this situation.

1.4 Outline of the Thesis

The structure of this paper is as follows. In chapter 2, the mission scenario, problem formulation, and model are proposed. Section 3 discusses the various estimation algorithm. Since EKF is used in this work, we formulate the EKF using bearing-only measurements. In addition, this chapter will discuss the Fisher information matrix-based scalar metric used for planning. Chapter 4 proposes the path and gimbal planning algorithm based on receding horizon method, which considers both communication and sensing. To verify the proposed algorithm, MATLAB numerical simulation is performed in chapter 5. Finally, the conclusion and future work is provided in chapter 6.

II Problem Description

This chapter describes the problem of multi-target tracking guidance for multi fixed-wing UAVs. By making the most of the information about the targets from each of UAVs, target states can be estimated. For the goal of this thesis, we assume that image processing, which contains identifying each target and finding the pixel coordinates of the centroid of the targets in the image, is already done. Then, the pixel location can be transformed into the corresponding bearing angle or relative unit vector by combining states of UAV.

Extended Kalman filter, which uses the bearing angle as measurements to estimate target states, will be described in Section 3. One of the purposes of this thesis is to maximize the information about targets. This purpose can be achieved by using information-theoretic methods. In order to plan the path and gimbal direction of UAVs that increase the information about targets, we must define the model of vehicle, target, sensor, and communication at first. Therefore, section 2.1 will summarize the scenario and the proposed algorithm in this thesis. And then Section 2.3 provides details of each model.

2.1 Problem Formulation
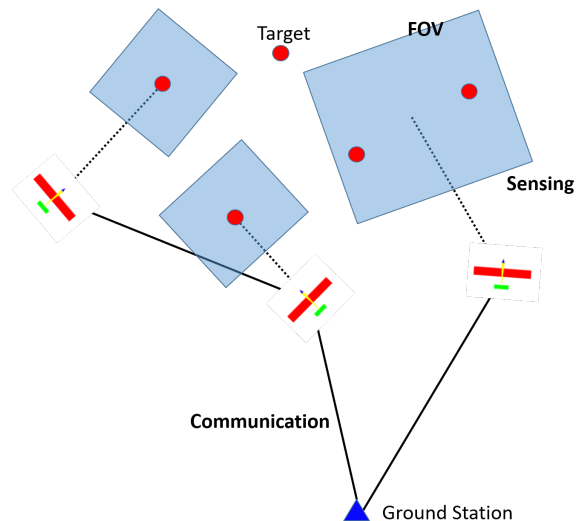
Figure 1: The scenario covered in this paper

We consider an urban environment with multiple targets and UAVs. Each of the UAVs' is equipped with a gimbal camera and a communication module. The camera provides pixel coordinates for the target through image processing and is converted into a bearing angle by combining with the UAV's status information. Also, it is assumed that information about the city is given in prior. Every target is road-bounded and has constant velocity.

The overall goal is to find the UAVs' path and gimbal command to track the multiple targets in urban environments with maintaining communication to the ground station. However, the communication between the UAV and the ground station is influenced by shading, fading, noise,

and other factors. It can seriously lessen the amount of received information. This paper explains realistic communication by using a packet erasure channel model. By incorporating this model into the plan, the UAV creates a path that acts as a communication relay to maintain communication with ground stations.

2.2 Model Description

UAV Dynamics Model

The UAV dynamics in this paper is derived from the general fixed-wing UAV model. For simplicity, the UAV is equipped with a flawless low-level flight controller, including the attitude angles and angular rates controller. So each UAV can follow the guidance input. In this paper, we assume that the UAVs flight on constant velocity and altitude. We use a constant altitude and coordinated turn model, which uses a roll angle as input. The equation is given by

$$\dot{p}_n = V_g \cos(\chi) \tag{1}$$

$$\dot{p}_e = V_g \sin(\chi) \tag{2}$$

$$\dot{\chi} = \frac{g}{\sqrt{V_g}} \tan \phi \tag{3}$$

$$\dot{\phi} = k_{roll}(u_1 - \phi) \tag{4}$$

where g is the gravitational acceleration constant, V_g is the ground speed of a UAV, χ and ϕ are course angle and roll angle, respectively. The parameter k_{roll} is the control gain, and u_1 is the desired roll command of each UAV, which is constrained by the following limits:

$$-\phi_{max} \leq \phi \leq \phi_{max} \tag{5}$$

This continuous dynamics model Equation 1-4 can be discretized by Euler integration method:

$$x_u(k+1) = x_u(k) + T_s(f_u(x_u(k), u_1(k))) \tag{6}$$

where T_s is the sampling time.

Target Dynamics Model

The target is assumed to move on the road in an urban environment, and it is assumed that one of three directions: forward, left, and right at each intersection is selected. Also, since the target's velocity is sufficiently lower than that of the UAV, the constant velocity model is used in this paper. The process noise of this model follows the acceleration, which regards a zero-mean Gaussian noise. The discrete model of target is given by:

$$x_t(k+1) = F(k)x_t(k) + G(k)w(k) \tag{7}$$

6

where $w(k) \sim N(0, Q(k))$ represents the white noise. The process covariance matrix $Q(k)$ is $diag(\sigma_{p_n}^2, \sigma_{v_n}^2, \sigma_{p_e}^2, \sigma_{v_e}^2)$. σ is the standard deviation related to states of the target about each axis. The state transition matrix $F(k)$ and the process noise matrix $G(k)$ are shown below:

$$F(k) = \begin{bmatrix} 1 & T_s & 0 & 0 \\ 0 & 1 & 0 & 0 \\ 0 & 0 & 1 & T_s \\ 0 & 0 & 0 & 1 \end{bmatrix} \tag{8}$$

$$G(k) = \begin{bmatrix} T_s^2/2 & 0 \\ T_s & 0 \\ 0 & T_s^2/2 \\ 0 & T_s \end{bmatrix} \tag{9}$$

Sensor Model

In this work, every UAV is equipped with a gimbaled camera to estimate the position of the target. After identifying the target through image processing, pixel coordinates of the target can be obtained, and the bearing angle between the UAV and the target can be obtained by combining the coordinates with the state information of the UAV. In this paper, it is assumed that image processing has already been performed. The sensor model used in this paper is quoted from [32]. Three coordinate systems are used to obtain the NED coordinates from the pixel coordinates of the target: camera frame, gimbal frame, and body frame. The rotation matrix from the gimbal frame to the camera frame is given by

$$R_g^c = \begin{bmatrix} 0 & 1 & 0 \\ 0 & 0 & 1 \\ 1 & 0 & 0 \end{bmatrix} \tag{10}$$

The rotation matrix from the body frame to the gimbal frame is given by

$$R_b^g = \begin{bmatrix} \cos\alpha_{el}\cos\alpha_{az} & \cos\alpha_{el}\sin\alpha_{az} & -\sin\alpha_{el} \\ -\sin\alpha_{az} & \cos\alpha_{az} & 0 \\ -\sin\alpha_{el}\cos\alpha_{az} & \sin\alpha_{el}\sin\alpha_{az} & \cos\alpha_{el} \end{bmatrix} \tag{11}$$

where α_{az} and α_{el} are the azimuth and elevation angles of the gimbal in regard to the UAV's body frame. The last one is the rotation matrix from Inertial frame to the body frame is given by

$$R_i^b = \begin{bmatrix} c_\theta c_\psi & c_\theta s_\psi & -s_\theta \\ s_\phi s_\theta c_\psi - c_\phi s_\psi & s_\phi s_\theta s_\psi + c_\phi c_\psi & s_\phi c_\theta \\ c_\phi s_\theta c_\psi + s_\phi s_\psi & c_\phi s_\theta s_\psi - s_\phi c_\psi & c_\phi s_\theta \end{bmatrix} \tag{12}$$

where $c_\phi \equiv \cos\phi$ and $s_\phi \equiv \sin\phi$. The ϕ, θ, and ψ are roll, pitch, and yaw angles of the UAV. The geometry of the camera frame is shown in Figure 2, where f and P are the focal length and scalar which converts pixel to units of Inertial frame. The position of the target in the camera frame is indicated by l_c. The projection of the target relative to the image plane is expressed in epsilon. The pixel position $(0, 0)$ corresponds to the center of the image, which is assumed to be aligned with the optical axis. The distance to the target is L. ϵ and f is in pixels. l is in units of Inertial frame. For simplicity, the image of the camera is assumed to be square. Therefore, if it is assumed that the width of the size of the image is M in pixels and the FOV of the camera is known as v, the focal length is calculated as follows:

$$f = \frac{M}{2\tan(\frac{v}{2})} \tag{13}$$

The relative position vector between the target and UAV is expressed as l, and the position of the target in the camera frame can be expressed as follows.

$$l^c = \begin{pmatrix} l_x^c \\ l_y^c \\ l_z^c \end{pmatrix} = R_g^c R_b^g R_i^b l \tag{14}$$

The coordinates of the pixel (ϵ_x, ϵ_y) and the size ϵ_s of the target in the image plane can be represented as

$$\begin{aligned} \epsilon_x &= f\frac{l_x^c}{l_z^c} \\ \epsilon_y &= f\frac{l_y^c}{l_z^c} \\ \epsilon_s &= f\frac{\check{S}}{l_z^c} \end{aligned} \tag{15}$$

where S is the size of the target in the camera frame. Then, the unit direction vector $\check{l}^c$ in the camera frame can be expressed as follows

$$\check{l}^c = \frac{l^c}{L} = \frac{1}{\sqrt{\epsilon_x^2 + \epsilon_y^2 + f^2}} \begin{pmatrix} \epsilon_x \\ \epsilon_y \\ f \end{pmatrix} \tag{16}$$

Here, L represents the distance between the target and the UAV in the inertial frame. Finally, using this relation and the rotation matrix, the azimuth and elevation between UAV and
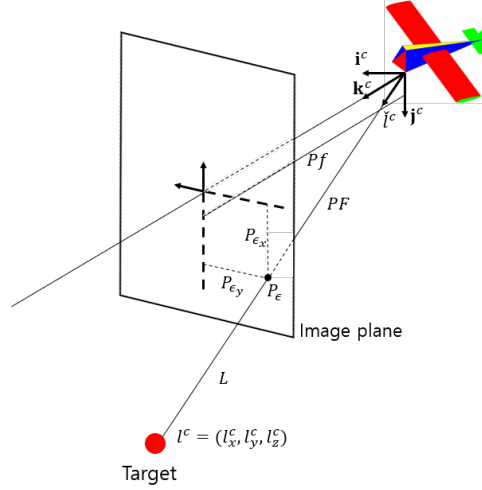
Figure 2: The geometry of camera frame.

target, which are measurements used in the Extended Kalman filter, can be obtained. These measurements can be obtained through the following equation.

$$\breve{l}^i = (R_i^b)^{-1}(R_b^g)^{-1}(R_g^c)^{-1}\breve{l}^c = \begin{pmatrix} \breve{l}_N^i \\ \breve{l}_E^i \\ \breve{l}_D^i \end{pmatrix} \tag{17}$$

$$\begin{pmatrix} \beta \\ \phi \end{pmatrix} = \begin{pmatrix} \tan^{-1}(\frac{l_E^i}{l_N^i}) \\ \\ \tan^{-1}(\frac{l_D^i}{\sqrt{(l_N^i)^2+(l_E^i)^2}}) \end{pmatrix} \tag{18}$$

where β and ϕ are azimuth and elevation, respectively. $\breve{l}^i$ is the unit vector in the Inertial frame. This equation is used as the measurement equation in EKF.

Second part of sensor model is gimbal dynamics. In this paper, we used pan-tilt gimbal and the equation of the gimbal motion is gien by

$$\dot{\alpha}_{az} = u_{az} \tag{19}$$

$$\dot{\alpha}_{el} = u_{el} \tag{20}$$

where u_{az} and u_{el} denote the control inputs for azimuth and elevation angles, respectively. To align the optical axis of the camera with the desired relative position vector l_d^i, we use the desired body-frame unit vector $\hat{l}_d^i$ as shown below

$$\dot{l}_d^i = \mathbf{p}_t^i - \mathbf{p}_u^i \tag{21}$$

9

$$\hat{l}_d^i = \mathbf{p}_t^i - \mathbf{p}_u^i \tag{22}$$

Next, select the commanded gimbal angles α_{az}^c and α_{el}^c by using the below relation

$$\check{l}_d^b = \begin{pmatrix} \check{l}_{xd}^b \\ \check{l}_{yd}^b \\ \check{l}_{zd}^b \end{pmatrix} = R_g^b(\alpha_{az}^c, \alpha_{el}^c) R_c^g \begin{pmatrix} 0 \\ 0 \\ 1 \end{pmatrix} \tag{23}$$

The Equation 23 means to rotate the focal axis from the camera frame to the body frame using the commanded gimbal angle. Solving for α_{az}^c and α_{el}^c gives the desired azimuth and elevation angles as

$$\dot{\alpha}_{az}^c = \tan^{-1}\left(\frac{\check{l}_{yd}^b}{\check{l}_{xd}^b}\right) \tag{24}$$

$$\dot{\alpha}_{el}^c = \sin^{-1}(\check{l}_{zd}^b) \tag{25}$$

Finally, the gimbal servo commands u can be selected as

$$u_{az} = k_{az}(\alpha_{az}^c - \alpha_{az}) \tag{26}$$

$$u_{el} = k_{el}(\alpha_{el}^c - \alpha_{el}) \tag{27}$$

where k_{az} and k_{el} are positive control gains.

Communication Model

To describe realistic communication links, this work uses the packet erasure channel model. The packet erasure channel model is a model that assumes that all packets are dropped when the signal-to-noise-ratio(SNR) Γ is less than a predefined threshold, and packets can be delivered only when the SNR Γ is above a predefined threshold. The SNR Γ_{ij} between UAV i and j is given by

$$\Gamma_{ij} = \frac{P_i G_{ij}}{N_j} \tag{28}$$

where $P_i > 0$ is the power provided to the antenna of communication module mounted in UAV i; $N_j > 0$ is the average power noise of a receiver, and G_{ij} is the channel gain. G_{ij} can be described by using the Rayleigh model.

$$G_{ij} = \frac{C_{ij}|h_{ij}|^2}{d_{ij}^\alpha} \tag{29}$$

where C_{ij} is a parameter that determines the effect of antenna gain and shading. h_{ij} means the multi-path fading. d_{ij} is the distance between UAV i and j . α is the propagation loss factor. If the threshold of SNR is defined as γ, the successful communication probability between two UAVs is given by

$$P_r^{ij}(\Gamma_{ij} \geq \gamma) = e^{-\frac{N_j \gamma d_{ij}^{\alpha}}{C_{ij} P_i}} \tag{30}$$

Equation 30 describes a realistic communication model. As explained above, when $\Gamma < \gamma$, packets between two UAVs are considered to be disconnected due to the dropping of each other. Contrariwise, when $\Gamma \leq \gamma$, the packet is considered to be transmitted according to Equation 30. If a packet has been transmitted, UAVs i and j are said to be connected to each other. Figure 3 shows the relationship between distance and probability P_{ij}.

Given some multihop path, the probability of successful transmission, $P_r(\text{path}_k)$, is obtained by assuming that each communication between UAV or ground station has an independent probability distribution, resulting in the following equation:

$$P_r(\text{path}_k) = \prod_{(i,j) \in path_k} P_r^{ij} \tag{31}$$
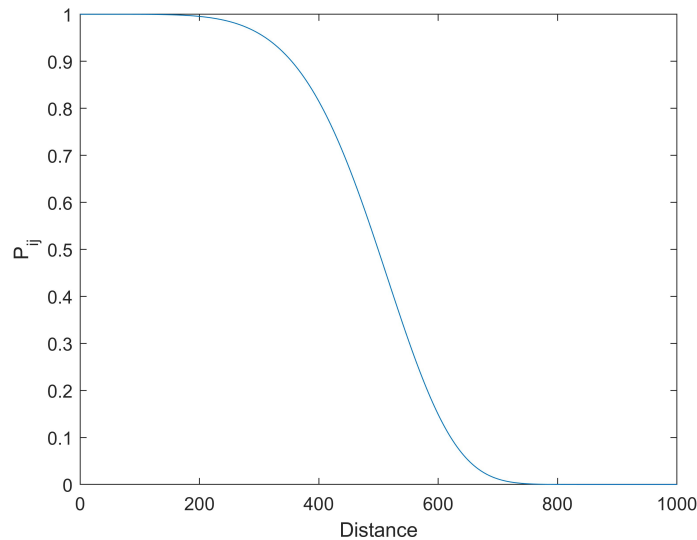

Figure 3: The relation between a successful transmission and distance according to Equation 30

In this paper, the communication routing algorithm selects the communication path with the most elevated probability of successful communication($P_r(\text{path}_k)$) between UAVs and the fixed ground station, $\text{path}_{0,k}^*$. This is formulated with the following equation. This optimization

problem can be solved by Dijkstra algorithm.

$$\text{path}^*_{0,k} = \text{argmax} \left[\prod_{(i,j) \in path_k} P_r^{ij} \right] \tag{32}$$

Equation 32 can be rewritten as

$$\text{path}^*_{0,k} = \text{argmin} \left[\sum_{(i,j) \in path_k} -\ln P_r^{ij} \right] \tag{33}$$

where k represents the order of each UAV. In Equation 33, $-\ln P_r^{ij}$ means each edge's weight, so this problem represents the shortest-path problem.
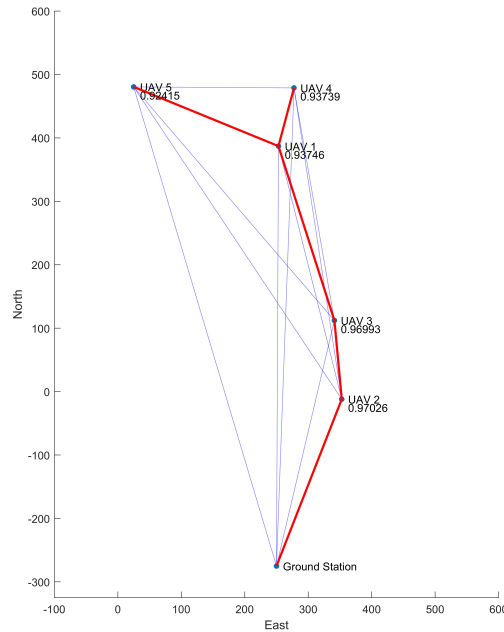
Figure 4: Example of communication path which maximizes the transmission probability between the UAVs and the ground station.

The example of the simulation result of Equation 33 is shown in Figure 4. The blue line represents every path between each UAV, and the red line represents the path that maximizes the transmission probability. The number under each UAV shows the transmission probability between the UAV and the ground station. This probability is used for planning purposes in the algorithms that will be introduced in Chapter 4.

III Target States Estimation

In order to generate the unmanned aerial vehicle's roll and gimbal commands, an algorithm is needed to estimate the state of the target. However, it is not easy to estimate the state of the target using bearing-only measurement. If the process contains nonlinearity and the parameter changes over time or there is a bias, the filtering algorithm may diverge.

Common algorithms used for target state estimation include KF, EKF, and particle filtering. In this chapter, the overall filtering algorithm will be briefly described, and the filtering algorithm used in this paper, Extended Kalman Filter, will be described in more detail. Finally, we will present the criteria for judging the estimated performance using the Fisher Information Matrix and explain how to use it for guidance.

3.1 Review of Estimation Algorithm

This chapter briefly describes some of the commonly used estimation algorithms. The algorithms considered are least squares estimation, Extended Kalman filter, and Particle filter. Kalman filter is considered for optimal estimation when dealing with LTI systems. When the system is nonlinear, Extended Kalman filter is used instead of the traditional KF. However, unlike a linear Kalman filter, if the state's initial estimation is incorrect or the process is misdesigned, the filter may diverge due to the nonlinearity of the system. Despite these weakness, the Extended Kalman filter is widely used because it can produce an appropriate estimation result.

Particle filter is more suitable for dealing with nonlinear systems, including non-Gaussian noise. The particle filter can be used instead of EKF, and optimal estimation can be made to increase the number of particles. However, as the number of particles increases, the computation time increases, and if the number of particles is too small, there may be problems in estimation. The following section describes the KF, EKF, and PF algorithms.

Least Squares Estimation

The least squares estimation algorithm operates to minimize the estimation error's square error for all parameters that need to be estimated. There are several types of the algorithm in LS, such as the traditional Batch least squares, Recursive least squares, and Extended least squares. The BLS algorithm is a widely used algorithm for states estimation. The main drawback of this algorithm is that it recalculates the ultimate estimate considering every prior data. This means that as the number of data increases, the computational complexity increases. The RLS algorithm improves this problem and shows more improved performance than the BLS algorithm using only the data in the current step at each time-step. However, since both algorithms do not work well in time-varying systems, ELS algorithms solve this problem.

Kalman Filter

Kalman filter is a recursive filter that estimates the state of a linear dynamics system based on measurements including noise, developed by Rudolf Kalman. Kalman filter is used in several fields, including computer vision, robotics, and radar. Kalman filter estimates the joint distribution of the current state variables based on current measurements.

The algorithm consists of two steps: prediction and update. In the prediction step, the value and accuracy of the current state variable are predicted. After the current state variable is measured, the current state variable is updated in the update step by reflecting the difference between the predicted measurement and the actual measurement based on the previously estimated state variable.

The traditional Kalman filter proposed by Rudolph Kalman can estimate the optimal state of a linear dynamics system. However, most practical systems have nonlinearity and may produce poor results in some systems. An Extended Kalman filter is developed to deal with this nonlinear system. However, unlike traditional KF, EKF is not an optimal estimation. If the initial estimation is incorrect or the process is misdesigned, it can be quickly diverged due to the nonlinearity of the system. Despite these drawbacks, EKF can perform well in many applications. However, if the system is highly nonlinear, many errors may occur in the linearization process of the nonlinear system, and the EKF may exhibit poor performance.

To solve this problem, Unscented Kalman filter (UKF), which can minimize linearization error by using a nonlinear equation as it is without a linearization process, is developed. To use the nonlinear equation as it is, Unscented Kalman filter uses an unscented transformation. The unscented transformation is a transformation that approximates the mean and variance of the posterior probability distribution by applying samples obtained through the mean and variance extraction of the prior probability distribution function to the transformation equation of the nonlinear probability distribution function. These samples are called sigma points, and the sigma points are selected by a deterministic method, unlike particle filters. Details on the Extended Kalman filter used in this paper will be described in Section 3.2.

Particle Filter

Kalman filter is an optimal estimation technique only when the probability distribution function of the system model and observation model is Gaussian, but it cannot be applied when non-Gaussian. Particle filter is developed for estimation when it is non-Gaussian, and particle filters are a technique that can be applied even when the probability distribution function does not follow a normal distribution.

Particle filter has the advantage of reducing linearization errors and not requiring complex Jacobian calculations such as EKF because there is no process for linearization nonlinear system functions. However, if the measurement has a singular value, the number of particles for accurate estimation may increase, and if the operation of extracting particles is not appropriate, it can

quickly diverge. Also, as the number of particles increases, the computation time may increase.

3.2   EKF for Vision-based Target States Estimation

Kalman filter is the most widely used and popular estimation algorithm and estimates the state of the LTI system based on measurements, including noise. This algorithm can produce optimal estimation results for the LTI system and is computationally efficient due to its recursive nature. Kalman filter assumes the linearity of the system model, but in reality, most of the models have nonlinearity. In this case, if Kalman filter is approximated and applied as it is, the result is not good. To solve this problem, an Extended Kalman filter is used. Extended Kalman filter, instead of the model's linearity assumption, assume the differentiability of the state transition function.

$$x_{k+1} = F_{k+1,k}x_k + w_k, \tag{34}$$

$$z_k = h(x_k) + v_k \tag{35}$$

where F is the state transition matrix of the system from k to $k+1$ and h is measurement model, respectively. Moreover, w_k and v_k denote the noise which is uncorrelated, Gaussian with zero-mean process and measurement and covariance Q_k and R_k respectively(i.e. $w_k \sim N(0, Q_k)$ and v_k $N(0, R_k)$). Kalman filter algorithm consists of two steps: prediction and update. In the prediction step, the value and accuracy of the current state variable are predicted. After the value of the current state variable is actually measured, in the update step, the current state is updated by reflecting the difference between the predicted measurement and the actual measurement based on the previously estimated state variable.

The prediction step of Kalman filter is shown below.

Prediction:

$$\hat{x}_{k|k-1} = F_{k,k-1}x_k + w_k, \tag{36}$$

$$\hat{z}_{k|k-1} = h(\hat{x}_{k|k-1}) \tag{37}$$

$$P_{k|k-1} = F_{k,k-1}P_{k-1|k-1}F_{k,k-1}^T + Q_k \tag{38}$$

We perform the update step in the information form of Extended Kalman filter which is is shown below.

Update:

$$P_{k|k}^{-1} = P_{k|k-1}^{-1} + \sum_{j=1}^{n_u} H_{j,k}^T R^{-1} H_{j,k} \tag{39}$$

$$\hat{y}_{k|k} = P_{k|k-1}^{-1}\hat{x}_{k|k-1} + \sum_{j=1}^{n_u} H_{j,k}^T R^{-1}(z_k - \hat{z}_{k|k-1} + H_{j,k}\hat{x}_{k|k-1}) \tag{40}$$

$$\hat{x}_{k|k} = P_{k|k-1}\hat{y}_{k|k} \tag{41}$$

where H_j is the measurement Jacobian. By combining the pixel coordinates of the target obtained using the gimbaled camera and the state information of the UAV, the bearing angle between the target and the vehicle can be obtained. The measurement model is given by

$$\beta = \tan^{-1}\frac{p_e - t_e}{p_n - t_n} = \tan^{-1}\frac{r_e}{r_n} \tag{42}$$

$$\phi = \tan^{-1}\frac{p_d - t_d}{\sqrt{(p_n - t_n)^2 + (p_e - t_e)^2}} = \tan^{-1}\frac{r_d}{\sqrt{(r_n)^2 + (r_e)^2}} \tag{43}$$

where $\mathbf{p}_k = [p_n \ p_e \ p_d]_k^T$ is the position of the UAV, $\mathbf{t}_k = [t_n \ t_e \ t_d]_k^T$ is the position of the target and $\mathbf{r}_k = [r_n \ r_e \ r_d]_k^T$ is the relative position vector between the UAV and the target. Then, its Jacobian with respect to the target states is

$$H = \frac{\partial \mathbf{h}}{\partial \mathbf{x}} = \begin{bmatrix} \frac{r_e}{r_n^2 + r_e^2} & 0 & \frac{r_n}{r_n^2 + r_e^2} & 0 \\ \frac{r_e r_d}{r^2(r_n^2 + r_e^2)} & 0 & \frac{r_n r_d}{r^2(r_n^2 + r_e^2)} & 0 \end{bmatrix} \tag{44}$$

(a) UAV and Target Position - 3D View   (b) Fisher Information
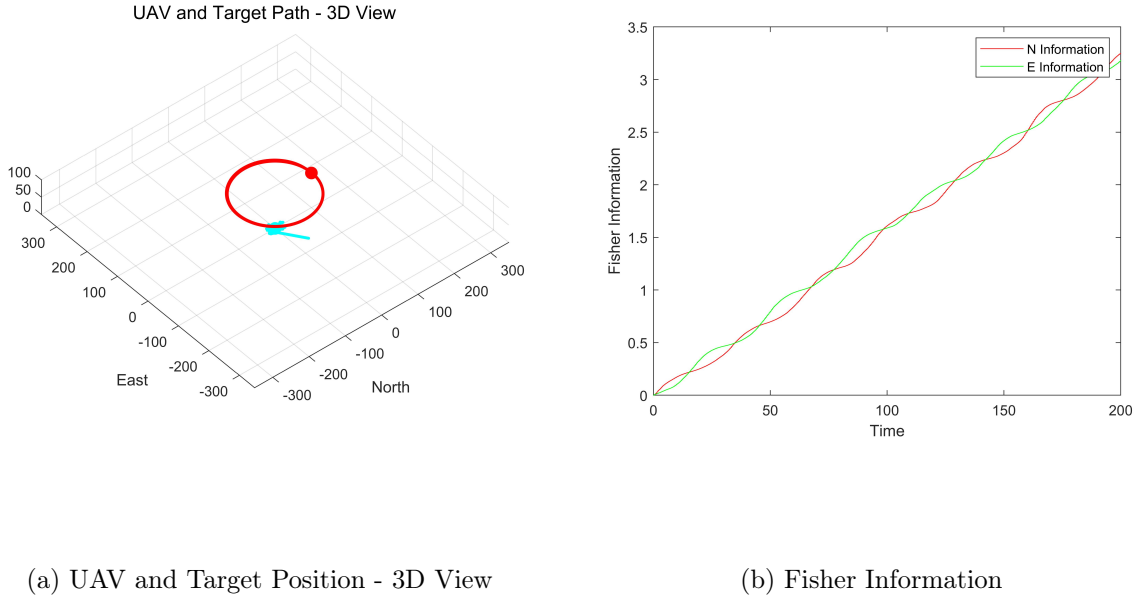
Figure 5: Results of EKF about the stationary target

Two cases of target tracking using EKF is considered in this chapter, containing stationary and constant velocity model. This section shows the results of EKF for these different cases. A 3-D simulation of the target estimation problem is used to test the result of Extended Kalman filter. The UAV path is selected to be circular above the target and the altitude is constant. The initial position of the target is initialized to (0,0), the camera FPS is set to 5 and the sensor's standard deviation is set to 5 deg. The results of EKF about the stationary target are shown

16

Figure 6: Error of stationary target states estimation results.

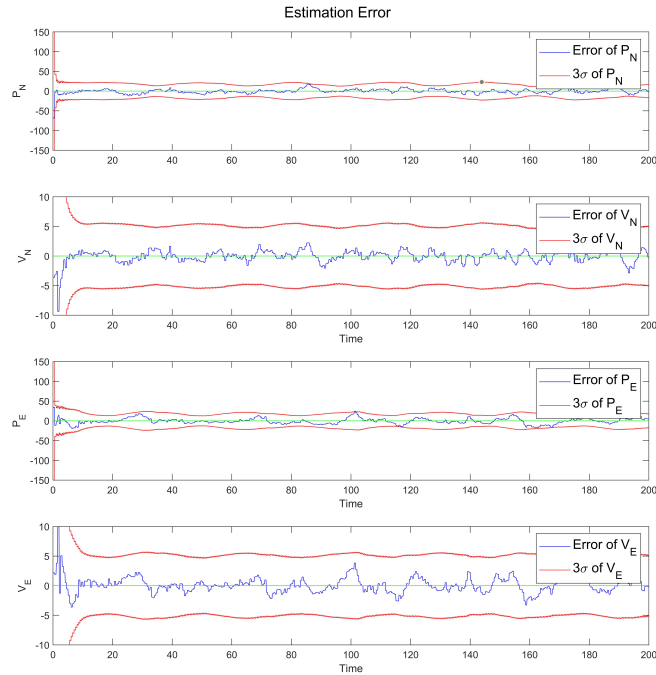in Figure 5-6. In Figure 5a, UAV and target paths are shown in 3D view. The red dot and circular curve represent the UAV's initial position and trajectory, and the cyan curve represents the estimated target position. Also, the blue star mark indicates the true position of the target. In the first case, it is assumed that the target is stationary at [0, 0]. The UAV's initial position is P_0=[0, 100] and its heading is pointing north.

The UAV is flying on the target in a circular trajectory, and except for the initial error, it can be seen that the estimated states of the target converge to the actual position [0,0] well. Figure 5b shows Fisher information about the position in the N and E directions. Through this graph, by following the circular path and obtaining continuous information about the target, it can be seen that the information about the position of the target in the N and E directions is continuously increasing. The results of estimation reflecting this result is shown in Figure 6. Figure 6 shows the estimation error of target states. Here, the red straight line represents the 3-σ error bound and the blue line represents the error of states. As can be seen from these graphs, it can be seen that the actual target state is estimated well. The uncertainty increases or is maintained at regular intervals because the sampling time of EKF is faster than the FPS of the sensor, so that only prediction is made in the absence of measurement. Also interesting is that the velocity of the target is estimated even though there is no measurement of the target's velocity. This is an advantage of Kalman filter, and it is possible to estimate the velocity because it is reflected in the estimation using the system model rather than merely using the previous estimate and measurement. In the case of the error bound of Figure 6, except when the

17

initial uncertainty is large, the sinusoidal pattern can be seen. This is because the measurement Jacobian is a function ofthe position of the UAV and the target, and the UAV is flying in a circular trajectory.
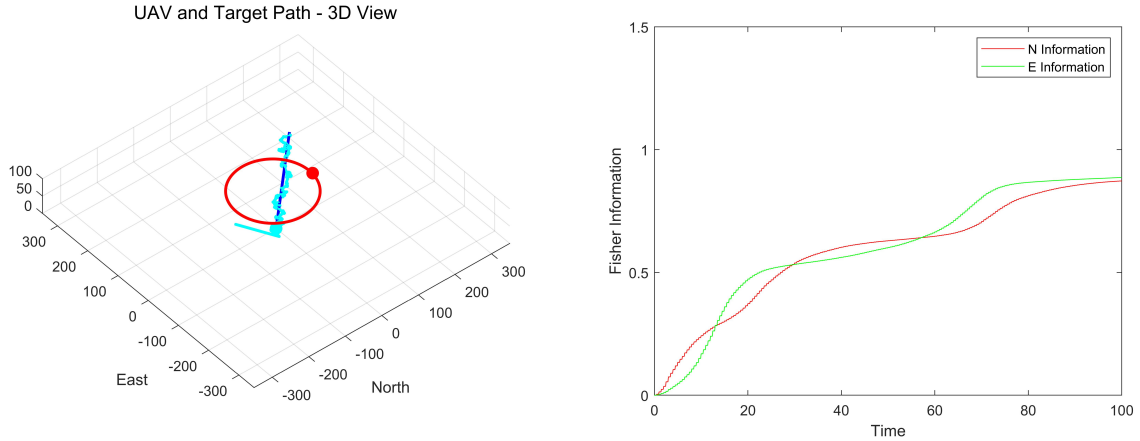
(a) UAV and Target Position - 3D View   (b) Fisher Information

Figure 7: Results of EKF about the moving target

The second case is a simulation for a target moving upwards to the right. The flight path of the UAV is the same circular trajectory as the first case. Figure 7a shows the trajectory of the UAV and target. The blue line represents the true trajectory of the target. Other graphs use the same notation as the graph in the first case. As can be seen from the simulation results, it can be confirmed that the estimation is comparatively good except when the initial error is large. However, it can be seen that the estimation error increases compared to the first case, which is a phenomenon that occurs because the target gradually moves away from the circular trajectory of the UAV. In fact, as shown in Figure 7b, it can be seen that Fisher information is reduced than the first case because measurement Jacobian is also a function of the relative distance between UAV and target. Therefore, as the distance increases, the information obtained about the target decreases relatively, and the estimation error also increases.
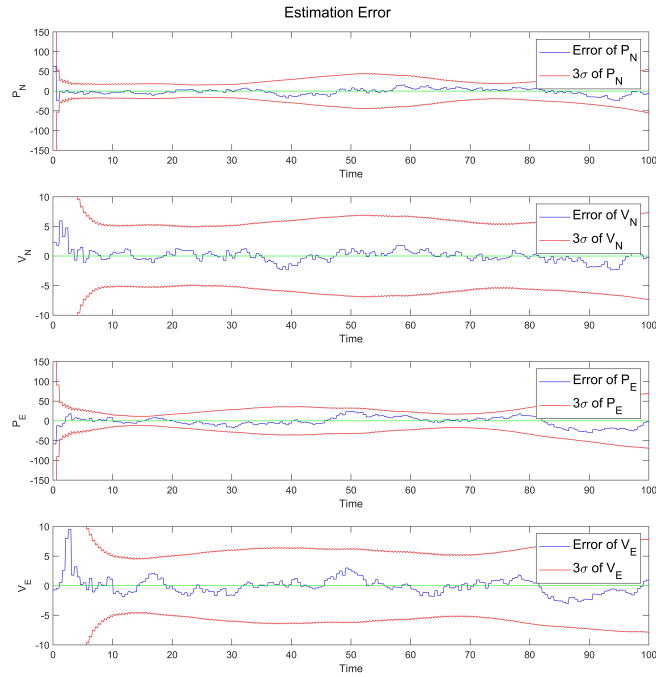
Figure 8: Error of moving target states estimation results.

3.3 Estimation Quality Metric

In this section, we will describe the scalar metric that can be used for planning. As mentioned in the previous section, since the measurement Jacobian of EKF is a function of the relative position between the UAV and the target, the estimation performance depends on the trajectory of the UAV and the target. Therefore, it is necessary to create an appropriate trajectory to increase estimation performance. This work aims to create a path and gimbal command that maximize information about the target while maintaining communication with the ground station. It is an important issue to select a proper quality metric to achieve the goal.

As stated by the Cramer-Rao lower bound theorem, the error covariance denotes the uncertainty correlated with the estimated states. Therefore, it should be minimized. In this case, the CRLB provides a lower bound for the uncertainty of a certain estimator. This can be expressed as follows

$$P_{k|k} = E[(\hat{x}_k - x_k)(\hat{x}_k - x_k)^T] \geq C_k = Y_k^{-1} \tag{45}$$

where x_k is the true target states to be estimated, $\hat{x}_k$ is the estimated target states, and $P_{k|k}$ is the error covariance matrix at time step k. The CRLB is denoted by C_k, and its inverse Y_k is the Fisher information matrix(FIM).

19

Since CRLB is formed founded on the physical characteristics of the system or the geometry related with the estimation, it provides a theoretical lower bound that any estimator can achieve. Therefore, by minimizing CRLB, the error covariance of the estimator can be minimized. Since FIM is the inverse of CRLB, this goal can be achieved by maximizing FIM.

FIM can be predicted by using the estimated target states and target motion model. From EKF, which is introduced in the previous section, we can compute the prediction of FIM through the following recursive form

$$\hat{Y}_{k+l|k+l} = (F_{k+l}\hat{Y}_{k+l|k+l-1}^{-1}F_{k+l}^T + Q_k)^{-1} + \hat{I}_{k+l|k+l} \tag{46}$$

where l is future step to be predicted and $\hat{I}_{k+l}$ is the prediction of the information matrix. The information matrix contains information about the target of all UAVs. Since this study considers camera LOS interference by buildings and communication with ground stations, the information matrix can be predicted by reflecting this through the equation as follows:

$$\hat{I}_{k+l|k+l} = \sum_{j=1}^{n_u} \alpha_{i,j}\beta_{0,j}\hat{H}_{j,k+l}^T R^{-1}\hat{H}_{j,l} \tag{47}$$

$$\hat{H}_{k+l} = \nabla_{\hat{x}_{k+l}}h(x_{u,k+l}, \hat{x}_{k+l}) \tag{48}$$

where x_u is predicted UAV's states in future step $k + l$, α is the binary variable to check if the target is in the FOV. β is the probability of transmission to the ground station. The predicted states of target and UAV are computed by using the model introduced in section 2.2. It can be reflected in the planning process while considering the constraints through Equation 47. For example, if there is no target in the image plane of the camera because it is obscured by a building, $\alpha_{i,j}$ becomes 0 and the information of the target becomes 0. Also, even if there is information, if $\beta_{0,j}$ is too low, it is multiplied like a gain to obtain a small amount of information.

However, since it is difficult to maximize FIM directly, it is requisite to define a scalar metric based on FIM and then perform optimization using it. One of the popular criterion is D-optimality criterion, which maximizes the determinant of FIM. The second criterion is A-optimality criterion. This criterion pursues minimize the trace of the inverse of the information matrix. The last criterion maximizes the minimum eigenvalue of the information matrix. And this criterion is called E-optimality.

IV Path and Gimbal Planning Algorithm Based on Receding Horizon

In this chapter, an information-theoretic multi-target tracking guidance algorithm that considers communication between the ground station and UAVs in an urban environment will be described. This study aims to create a roll command and a gimbal direction command for the UAV that maximize target information while maintaining communication with ground stations in an urban environment. To achieve this goal, several processes are run distributedly on each UAV. This chapter is organized as follows.

First, an overview of the proposed algorithm is shown. The overall operation of the algorithm and the shape of the objective function will be briefly described. In the second section, the objective function used in the proposed algorithm is formulated in detail. In the third and fourth sections, cluster allocation and weight calculation using DBSCAN clustering results will be described. And in the last section, we will discuss how to consider communication with ground stations.

4.1 Overview
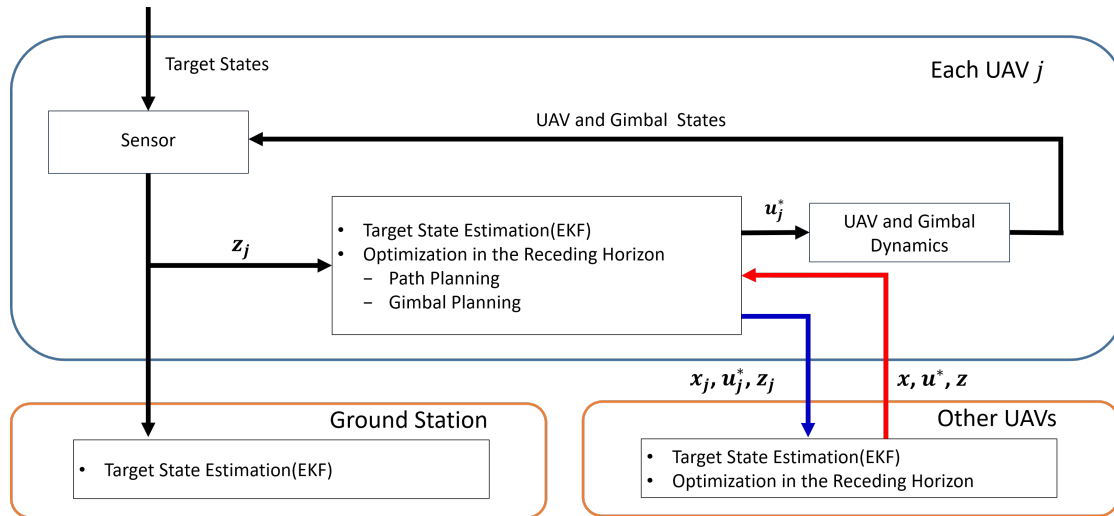
Figure 9: Overall process of the proposed algorithm.

In this section, a brief description of the receding horizon technique and the overall process of the algorithm is described. The receding horizon method is one of the methods to control the system while considering a series of constraints. First, a time to be predicted is set, and a control action is created by taking into account the future cost and various constraints such as the dynamics of the UAV during this time and information on the environment. The best advantage of this technique is that it optimizes using information from the current time step and considers the future time step. It can continue planning by recursively optimizing while considering a finite time horizon.

In this study, based on the information on the UAV and target dynamics and the urban environment for a specific time to be predicted, the UAV roll angle and gimbal direction commands are generated to maximize the information about the target while maintaining communication with the ground station. The objective function for this is proposed, and the receding horizon technique is used to maximize this. We will discuss in detail the objective function proposed in Section 4.2. In addition, the input command is discretized to reduce the computation time, and the control is repeatedly at each control cycle performed using the first value of the planned series of inputs. The proposed algorithm using the receding horizon technique is distributed in each unmanned aerial vehicle, and for this purpose, the state information of each unmanned aerial vehicle and the measurements of the target are exchanged throug a communication module between the UAVs. The proposed algorithm follows the process shown in Figure 9. First, each target is clustered through the DBSCAN algorithm using the current estimated target location. Second, using the clustering result, the cluster is allocated to each UAV, and the weight of each cluster is calculated. At this time, the error covariance matrix of the estimation result is used to give priority to clusters with high uncertainty and based on this, the traveling distance between the current location of UAV and the cluster's central location is minimized. Finally, planning based on the receding horizon method is performed based on other UAVs' status information and the planned input. Also, during the estimation process, the measurements are transmitted from other UAVs and reflected in the estimation, and then this process is recursively performed.

4.2 Objective Function

To achieve the goal of this study, the following objective function is proposed that can reflect information such as communication with ground stations and urban environment.

$$
J = \sum_{k=1}^{m} (w_1 J_{1,k} + w_2 J_{2,k}) \\
w_1 + w_2 = 1
$$

(49)

J_1 is a sensing and communication part, and J_2 is a part to approach a target that cannot be sensed. The variable m represents the time horizon step of the receding horizon method, and the objective function of each step is summated to consider multi-steps. w_1 and w_2 represent the weights reflecting the current uncertainty and determine which objective function to focus on between J_1 and J_2. J_1 is formulated using Fisher information matrix to reflect sensing and communication, and J_2 allows UAVs to approach targets with high uncertainty as quickly as possible. The weight is multiplied in front of each term, and it is variable to reflect the current situation. In general, J_2 is not used for path planning using FIM. However, if the measurement for the target is not obtained during the prediction process of receding horizon planning, that target will be missed. Therefore, J_2 is introduced to solve this problem. By introducing J_2, the UAVs can reach the target and keep track of it before the uncertainty becomes too high. J_1 and J_2 are composed as follows.

$$J_1 = -\prod_{i=1}^{n_t} \left(\left(P_{k+1|k}^{-1} + \sum_{j=1}^{n_u}(\alpha_{i,j}\beta_{0,j}H_{ij}^T R^{-1}H_{ij}) \right)^{-1} \right) \tag{50}$$

$\alpha_{i,j}$: Binary variable to check FOV

$\beta_{0,j}$: Probability of successful transmission between ground station

$$J_2 = \frac{1}{D_k} \tag{51}$$

D_k : Distance between UAV and selected target

In Equation 50, n_t and n_u represent the number of targets and UAVs, respectively. J_1 is formulated using the trace of the inverse of Fisher information matrix. In order to reflect the measurement of all UAVs for a certain target, the information matrix of each UAV is calculated and added together. In addition, $\alpha_{i,j}$ and $\beta_{0,j}$ multiplied in front of each UAV's information term are terms that consider the FOV between the UAV and the target and communication with the ground station, respectively. For $\alpha_{i,j}$, it is 0 if the target is outside the sensing range or is not in the FOV by a building, and 1 otherwise. By using this term, sensing in an urban environment can be considered. In the $\beta_{0,j}$, it represents the probability of successful transmission between the ground station and the each UAV obtained using the packet erasure channel model and is multiplied like a weight to reflect communication. The communication successful probability between the ground station and UAV, $\beta_{0,j}$, is calculated is described in detail in Section 2.2.

The second term, J_2, is formulated using the relative distance to the target with high uncertainty within the assigned cluster. In the prediction step of receding horizon, the relative position is calculated for each step, and the command to minimize the distance to the target is generated using this. This term does not always work. It works according to w_2 which is calculated according to the current target uncertainty. For example, if the target's uncertainty remains below the threshold, w_2 is kept at 0, and a command is generated that considers sensing and communication without J_2. In this case, the uncertainty of the target increases, and the target can be considered by J_2. In general, in a study related to path planning using Fisher information, only J_1 is used. However, if the measurement of a target cannot be obtained in the prediction step of the receding horizon with the only use of J_1, a situation in which the target is missed may occur. J_2 is introduced to solve this problem.

4.3 Optimization Strategy

Using the proposed objective function in section 4.2 to plan trajectory and gimbal command of UAV over the finite time horizon, the solution of the following optimization problem is required.

$$(\mathbf{u}^*_{1,k+1:k+m}, \mathbf{u}^*_{2,k+1:k+m}) = \mathrm{argmax} J \tag{52}$$

where $\mathbf{u}^*_{1,k+1:k+m}$ and $\mathbf{u}^*_{2,k+1:k+m}$ is the desired roll angle command and gimbal direction command, respectively, and are series of inputs during the future time that maximizes the objective function.

The optimization is performed with receding horizon method over the control frequency. Future cost is calculated over the finite time horizon step m to relax the computational burden in each UAV. This time step can be set to fit the hardware specification of the UAV.

This algorithm is done in a distributed fashion. Each UAV independently performs this algorithm and plans based on the planned path and the acquired information by other UAVs. Through this algorithm, a series of inputs are generated during finite time steps that improve communication and sensing performance. And use the first value of this input during the control frequency.

4.4 DBSCAN Clustering

In this study, DBSCAN algorithm is used for efficient UAV path planning. DBSCAN Clustering (Density-Based Spatial Clustering of Applications with Noise) is a density-based clustering algorithm that performs clustering based on the density of a given data set. In this work, the data to be considered is position information of randomly moving targets. Therefore, the shape of the cluster depends on the path of the target and the number of clusters is also variable, so the density-based DBSCAN algorithm is more suitable than the K-means clustering algorithm.
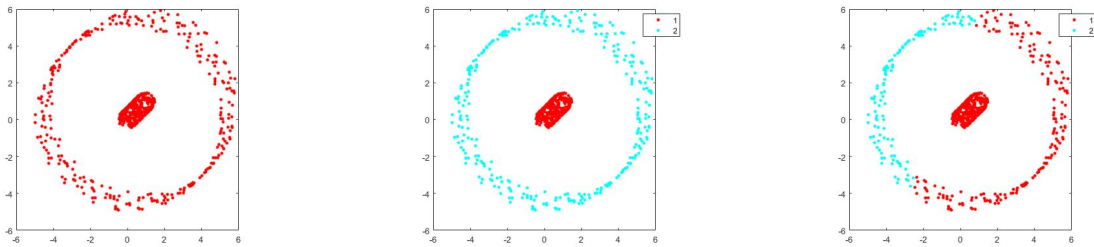
| (a) Original Data | (b) Results of DBSCAN clustering | (c) Result of K-means clustering |

Figure 10: Comparison of results between DBSCAN and k-means clustering

The advantage of this algorithm is that, unlike K-means clustering, this algorithm does not need to specify the number of clusters and automatically finds the number of clusters. In addition, since noisy data can be classified while performing clustering, the degradation of clustering performance due to outliers can be mitigated. In addition, clustering is performed based on density, so we can find clusters that have no shape. On the downside, it has quadratic time complexity, unlike K-means clustering, which has linear time complexity in the number of data. In addition, the clustering result varies according to the order in which data is input and the distance measurement method used by the algorithm. Finally, if the characteristics of the data are not known, it is difficult to set an appropriate hyper-parameter of the algorithm.

In this study, the location of the target is used as data, and the target moving along the road

is assumed, so if the distance between the data is less than one block of the city, the target is set to belong to the same cluster. In addition, since the number of targets is small, the calculation time is not large even when the DBSCAN algorithm is used.

The objective function proposed in Section 4.2 creates a path to the target when the uncertainty of a target becomes too large. In this case, if a target with high uncertainty is gathered on one side, an inefficient path is formed because all UAVs move to the target. In order to alleviate this phenomenon, DBSCAN algorithm is introduced and using this clustering result, each UAV is allocated and w_2 is calculated.

4.5 Cluster Allocation and w_2 Calculation

This section describes a method of allocating a cluster to each unmanned aerial vehicle and calculating w_2 based on the clustering result. First, in order to designate the priority of the cluster, the uncertainty of the cluster is obtained by using the error covariance matrix of targets belonging to each cluster. The covariance matrix of each target can be obtained using Extended Kalman filter introduced in Section 3 and quantified using determinant, one of the scalar metrics of this value. After sum all of the scalar metrics of each target, priorities are determined based on the result. The higher priority of the cluster, the more likely it is that UAVs will be allocated. Finally, each UAV is allocated in order of priority and is allocated to each UAV in a combination that satisfies the minimum traveling distance between the centers of the cluster. At this time, because the DBSCAN clustering algorithm returns only the cluster and the targets included in the cluster, the center of the cluster is calculated using the average of the target positions. The pseudo-code of the allocation algorithm is shown in Algorithm 1 and Algorithm 2. This is similar to [29].

Algorithm 1 shows the overall algorithm process, and Algorithm 2 shows each function of Algorithm 1. First, calculate Info and w_2 of each cluster in lines 1 2 of Algorithm 1. N_c and N_u are the number of clusters and UAVs, respectively, and $P_{i,j}$ represents the covariance matrix of the target i belonging to the j-th cluster. Calcul_Information uses the covariance matrix of each target as input and returns Info. Info represents the amount of information in each cluster. And Calcul_Weight2 function uses Info as input and calculates w_2 through Equation 53. In order to distribute the load when several UAVs are allocated to the cluster, the summation of the determinant of an error covariance matrix is divided by the number of UAVs in each cluster, N_n^c.

The form of this function is like a sigmoid. The variable 'a' is a design parameter that determines the sensitivity of uncertainty change. Depending on this value, it is possible to set whether w_2 changes rapidly or gradually. Since the input of this function is a determinant of an error covariance matrix, the weight is changed depending on the uncertainty. The lower and upper limits of the function is specified as 0 and 0.9, respectively. In addition, the uncertainty and w_2 of each cluster are calculated through Equation 53 and reflected in the planning. If the overall target uncertainty is low, w_2 is maintained at 0, and the planning proceeds by J_1. On

---

Algorithm 1 Cluster Allocation Algorithm.

Calcul_Info_Weight2

if $N_c \geq N_u$

  NoC_Greater_NoU

else

  NoC_Less_NoU

  $res = N_u - N_c$

  if $res == 1$

    Assign the cluster with higher uncertainty to UAV.

  else

    while Every UAV have not been assigned

      if $N_c > res$

        NoC_Greater_NoU

      else

        NoC_Less_NoU

      end

    end

  end

end

Algorithm 2 Each function for Algorithm 1

---

function Calcul_Info_Weight2($P_{i,j}$)

  for $i = 1 : N_c$

    Info$(i) = 0$;

      for $j = 1 : N_t^c$

        Info(i)=Info(i)+det$(P_{i,j})$

      end

    Calculate w_2 through Equation 53

  end

  return Info, w_2

end

function NoC_Greater_NoU(p_c, p_u^{na}, N_u^{na}, Info)

  Select the top N_u^{na} clusters with larger uncertaisnty

  $v = $ permutations(Center of clusters)

  for $i = 1$:size(v)

    Average of traveling distance of the UAVs to the center of clusters

  end

Select a permutation that satisfies the minimum traveling distance

return Assigned cluster for UAVs

end

function NoC_Less_NoU(p_c, p_u^{na}, N_u^{na}, Info)

v = permutations(N_u^{na}, N_c)

for $i = 1$:size(v)

Average of traveling distance of the UAVs to the center of clusters

end

Select a permutation that satisfies the minimum traveling distance

return Assigned cluster for UAVs

end

---

the contrary, if the uncertainty of the target is high, w_2 will gradually increase depending on uncertainty, and planning is dominant by J_2. At this time, since the upper limit is 0.9, sensing and communication are also being considered by J_1 with other weight. Based on this, the path is selected by J_2, and the gimbal direction command is selected by J_1. Since the calculation of w_2 is performed before the receding horizon based planning begins, it is always possible to calculate the weight that reflects the current situation. Therefore, using this method, even if information about a specific target is not obtained in the prediction step, targets with too high uncertainty can also be considered.

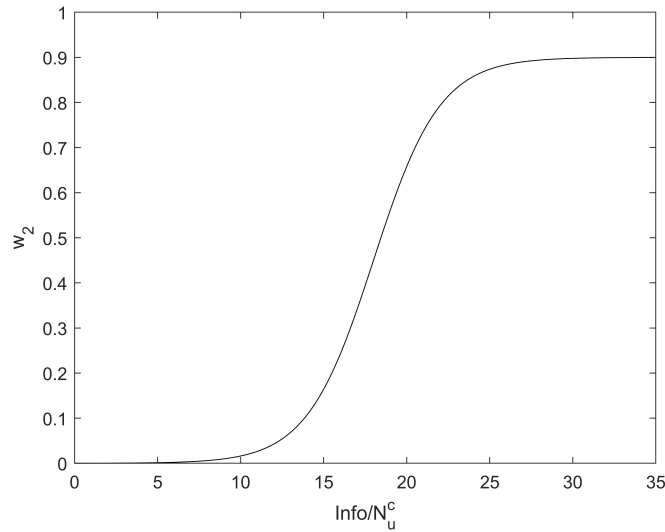$$w_2 = \frac{0.9}{1 + e^{a(\text{Info}/N_u^c))}} \tag{53}$$

Figure 11: w_2 calculation function. The upper bound is limited to 0.9 for gimbal planning.

Lines 4 to 20 show the process of allocating each UAV to each cluster. The algorithm proceeds until all UAVs are assigned to a cluster. When N_c is greater than or equal to N_u, NoC_Greater_NoU function is used, and NoC_Less_NoU is used otherwise. The inputs of the two functions are the center coordinates of the cluster (p_c), the locations of unallocated UAVs (p_u^{na}), the number of unallocated UAVs (N_u^{na}), and the amount of information in each cluster(Info). Basically, both functions select the combination that minimizes the traveling distance. However, there are some differences in the way the possible allocation combinations are calculated. The former function finds a combination that selects as many clusters as the number of unallocated UAVs. The latter function finds a combination that selects unallocated UAVs as many as the number of clusters.

V   Numerical Simulation

Numerical simulations of various cases are performed to evaluate the proposed algorithm. First, we will show the results with and without β and J_2 in various environments in order to check the role of each part of the objective function.

Two main scenarios are considered in this chapter. The first scenario will show the simulation results of the generally widely used FIM-based planning scheme and its problems. Moreover, we tested the features of J_2 that we introduced to solve this problem. Second, it shows the result according to the presence or absence of β, which is introduced to consider communication.
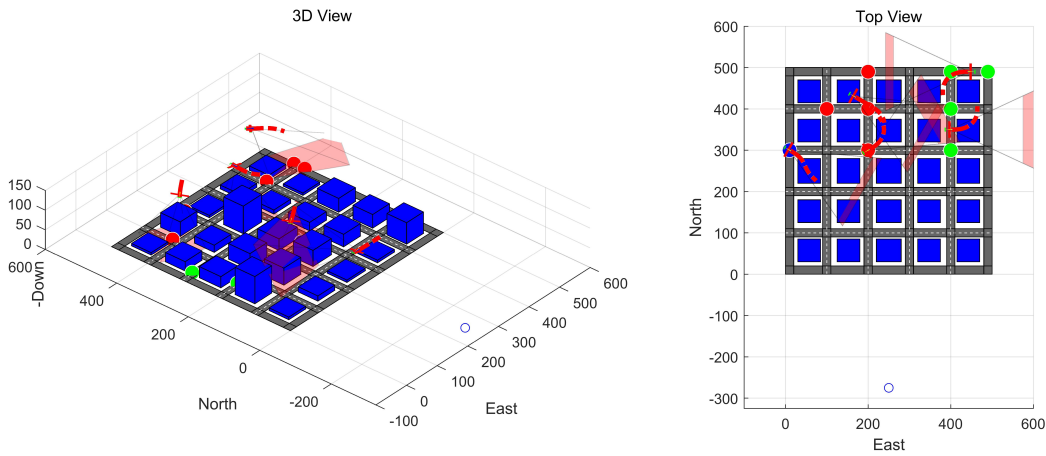

Figure 12: Example of simulation environments.

The overall simulation environment is as follows. First, in the case of the UAV, a fixed-wing UAV equipped with a gimbaled camera is used. The camera's sensing range is 200 meters, and each UAV maintains a constant velocity and altitude. In addition, to prevent a collision, it is assumed that each UAV has a different altitude and flies above the maximum height of the building. Also, it is assumed that the target moves at a constant velocity on the road, and the velocity of each target is randomly distributed between 2 and 5 m/s. In addition, it is assumed that the initial position of the target is known and that uncertainty is large enough. In the case of an urban environment, a square map of 500m width with 25 buildings is used, and the height of each building has a random value between 10 and 70m. The standard deviation of system noise and measurement noise is set to $2.5 m/s^2$ and 5 deg. Finally, since the target search is not considered in this paper, it is assumed that the number and the initial position of the target are known and its uncertainty is high.

5.1 Scenario I : Effect of J_2

In this section, the simulation result with and without J_1 in the proposed algorithm is shown. This result is divided into three cases. The first and second cases consider a single UAV and a single stationary target. These cases compare the results of introducing J_2 in a special situation where target tracking is not possible when only J_1 is used. In the third case, the number of UAVs and targets is 2 and 3, respectively, and the urban environment is considered. Also, in this section, it is assumed that a flawless communication module is mounted on the UAV in order to analyze the problem when only J_1 is used from the point of view of sensing.
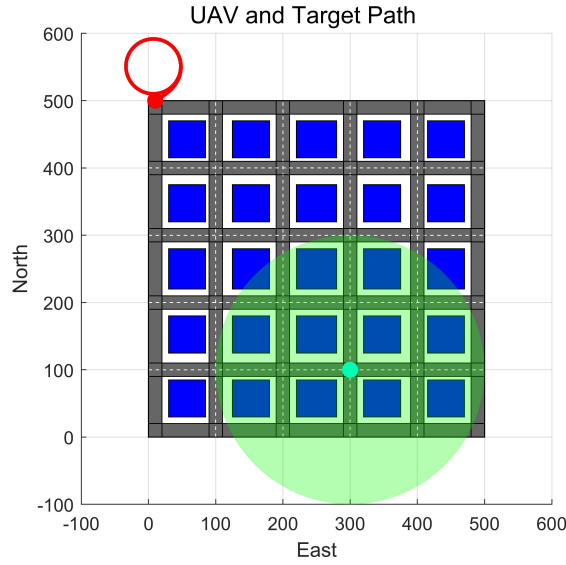

Figure 13: Target visibility area and trajectory of UAV without J_2

Figure 13 shows the simulation results of the first case. In Figure 13, the red curves and points represent the UAV's trajectory and initial position. Also, the cyan point represents the target's location, and the green circle represents the visibility area of the target. So, if the UAV is in this green circle and a building does not obstruct the camera's line-of-sight, UAV can get information about the target from the camera.

As can be seen from the simulation results, the circular trajectory is generated in this situation. In this situation, UAV always chooses the first input because no matter what input is used in the receding horizon method's prediction process, information about the target cannot be obtained. Also, since information about the target cannot be obtained, the uncertainty of estimates continues to increase. This is a problem that occurs when using only FIM.

The second case shows the role of J_2 introduced to solve this problem. Simulation is performed under the same conditions as the environment shown in the first case, and the results are shown in Figure 14.

Figures 14a and 14b show the UAV path and urban environment in 3D and top view. Unlike the result of the first case, by introducing J_2, it is confirmed that the UAV tracks the target

(a) Trajectory - 3D View
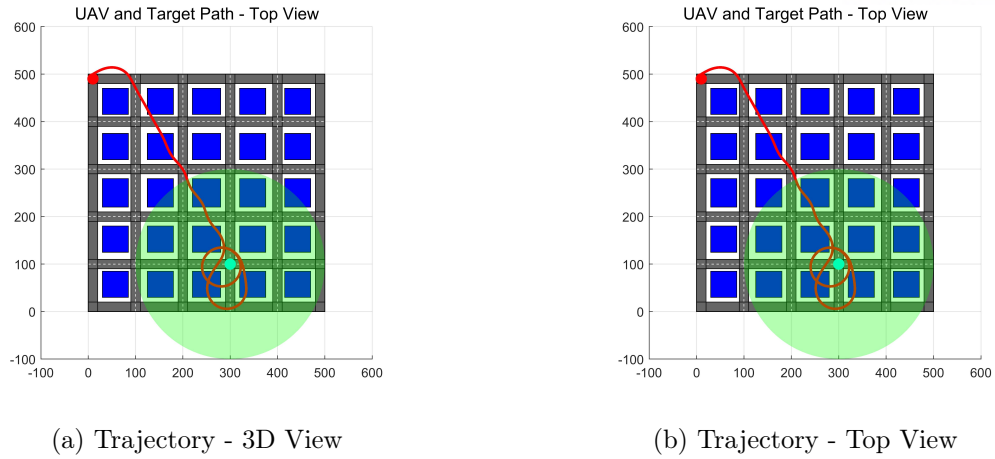
(b) Trajectory - Top View

Figure 14: UAV trajectory with $J_1 + J_2$

even in situations where uncertainty continues to increase because it is outside the sensing range or is obstructed by a building. Figure 15 shows the w_2. As shown in the graph, since the UAV enters the green circle area from 18 seconds and acquires the measurement of the target, it can be seen that the uncertainty is rapidly decreased. As a result, w_2 rapidly converges to 0, and a path for obtaining more information is created using only J_1 within the green circle area where the information of the target can be obtained.
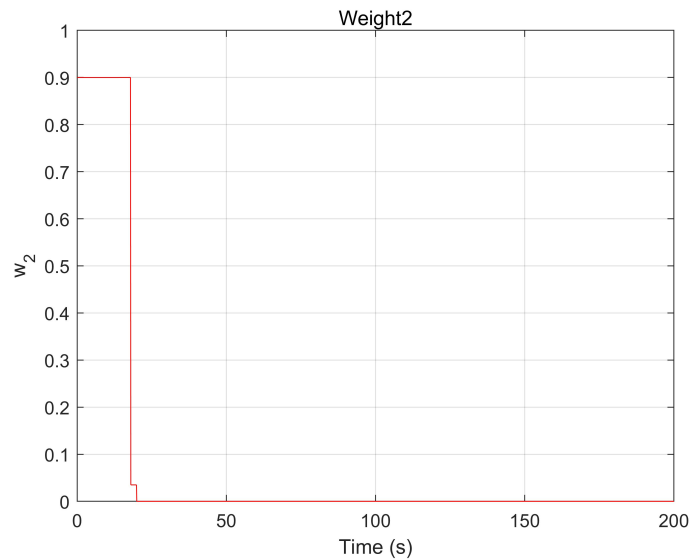

Figure 15: w_2 graph with $J_1 + J_2$

The third case shows the results of numerical simulation in 70 different environments to confirm the advantages of the proposed algorithm. The situation in which two UAVs track three targets in an urban environment is considered, and the mission success rate is compared for each camera sensing range. The initial location of the target is randomly selected from one of 36 intersections, and each UAV is initialized at a random location near the target. It is also

31

Parameter	Value	Parameter	Value
N_{UAV}	2	Building Heights	10~70 (m)
N_{Target}	3	Sensing Range	150~300 (m)
V_{UAV}	15 (m/s)	Control Freq	2 (sec)
V_{Target}	2 (m/s)	Camera FPS	0.1 (sec)
$N_{Building}$	25	Camera FOV	50 (deg)

Table 1: Parameter List

assumed that the initial position of the target is known. The main parameters used in the simulation are summarized in Table 1.
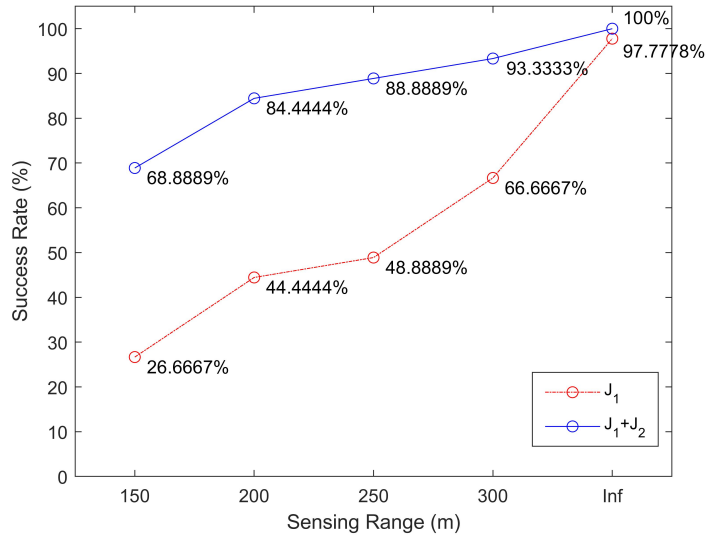

Figure 16: Comparison of success rate

Figure 16 shows the success rate of the target tracking mission according to the sensing range in the 70 numerical simulations. If the maximum value of uncertainty exceeded 500 meters, which is the width of the city map, it was judged as a failure. The red line is the result of using the objective function J_1 formulated by using FIM, and the blue line is the result of $J_1 + J_2$(Proposed).

As shown in Figure 16, it can be seen that the success rate is much higher when the proposed objective function is used than when only J_1 is used. Since the location of the target is entirely randomly distributed, in the case of the objective function using only FIM, it can be seen that the shorter sensing range, the drastically lower the success rate. However, in the case of using the proposed algorithm, since a path to the target's estimated position with high uncertainty is generated when the uncertainty is greater than the threshold, it is confirmed that the success rate increases even in such challenging environments.

5.2   Scenario II : Communication

This section will show the difference between the presence and absence of the parameter β considering the communication between the fixed ground station. This section is divided into three parts. First, the results when communication is considered or not considered for two UAVs and a single target in an urban environment are compared in case 1 and 2. Second, to evaluate the performance of the algorithm proposed in Chapter 4, the results of 70 numerical simulations will be shown. In this simulation, 5 UAVs were used to maintain communication with the ground station far from the city while tracking 9 targets distributed throughout the map.
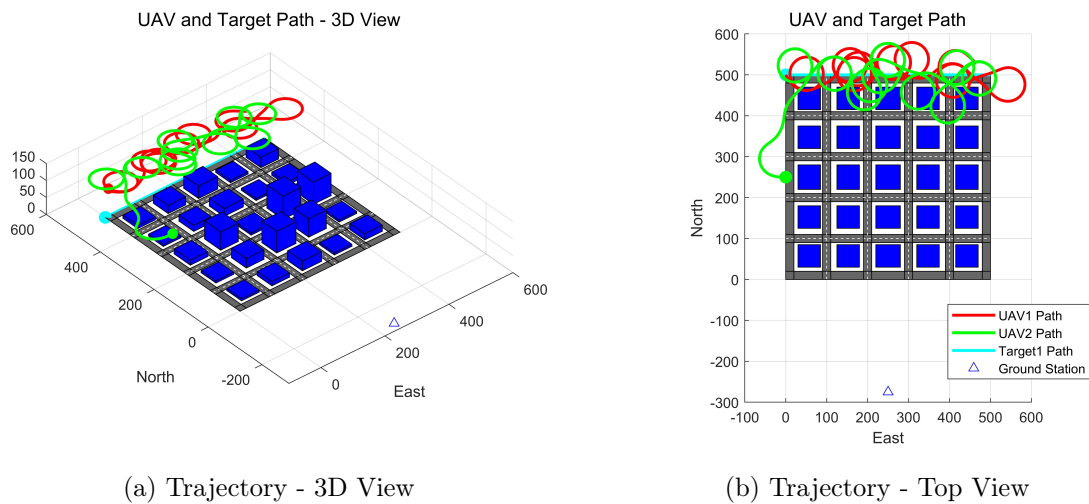

(a) Trajectory - 3D View

(b) Trajectory - Top View

Figure 17: Trajectory without considering Comm.

(a) Exchanged packets between the ground station (b) Trace of Fisher information at the ground station
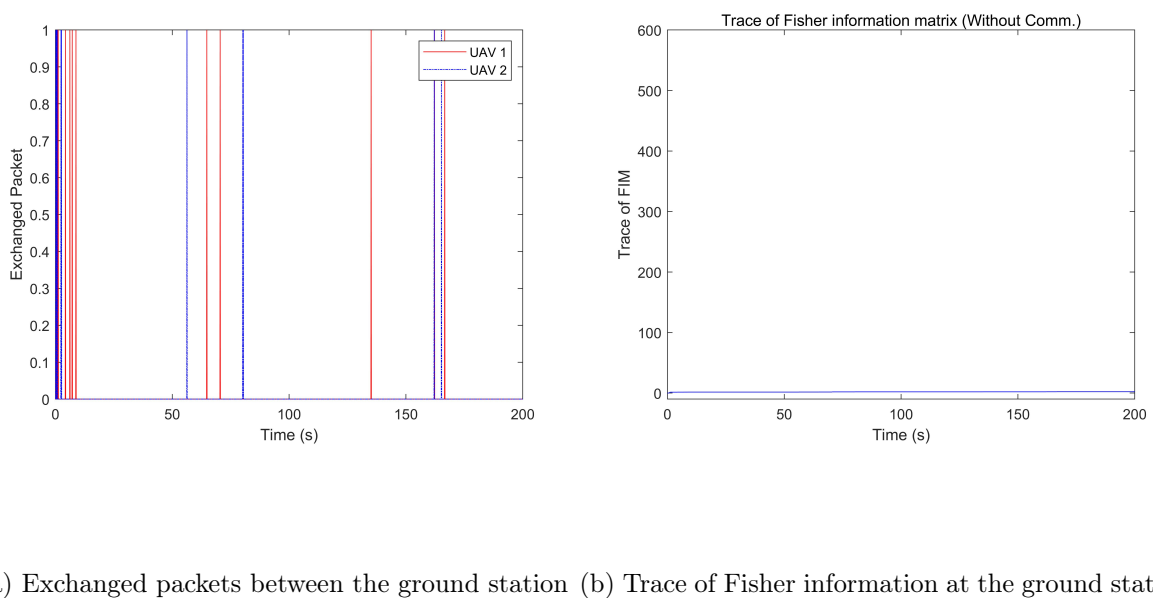
Figure 18: MATLAB simulation results without considering Comm.

In this section, the simulation results will be shown when communication with ground stations is not considered. The initial positions of UAVs are [250, 0] and [490, 0], respectively, and the initial positions of the target are [490, 0]. The target is moving to the right at a constant velocity of 2.5m/s. The ground station is also located at [-275, 250] to consider the target far from the ground station. It is also assumed that the location of the initial target is known, and the uncertainty is high.

Figure 17 and 18 show the simulation results. Figure 17 shows that the red, green, and cyan lines represent UAVs' trajectories and targets, respectively. Also, the blue triangle means the location of the ground station. Also, it shows that the trajectory of every UAV is formed around the target because communication with the ground station is not considered. Initially, since the uncertainty of the target's estimates is high, a trajectory is created to get as close to the target as possible. When the uncertainty is lowered by sensing the target, a trajectory to obtain the maximum information is created by J_1. Figure 18a shows the packets exchanged between the ground station and each UAV. The value 1 means that packets are exchanged, and 0 means that packets are not exchanged. Figure 18b appears the cumulated sum of trace of the Fisher information over every time step. In this case, it can be confirmed that communication is not possible because the distance to the ground station is far(See Figure 18a). Therefore, since the information about the target is not transmitted to the ground station, it can be seen that the Fisher information does not increase. Therefore, it can be seen that Fisher information continues to accumulate. At this time, we can see that Fisher information increases rapidly at an instant because the information increases rapidly when the UAV is directly above the target.

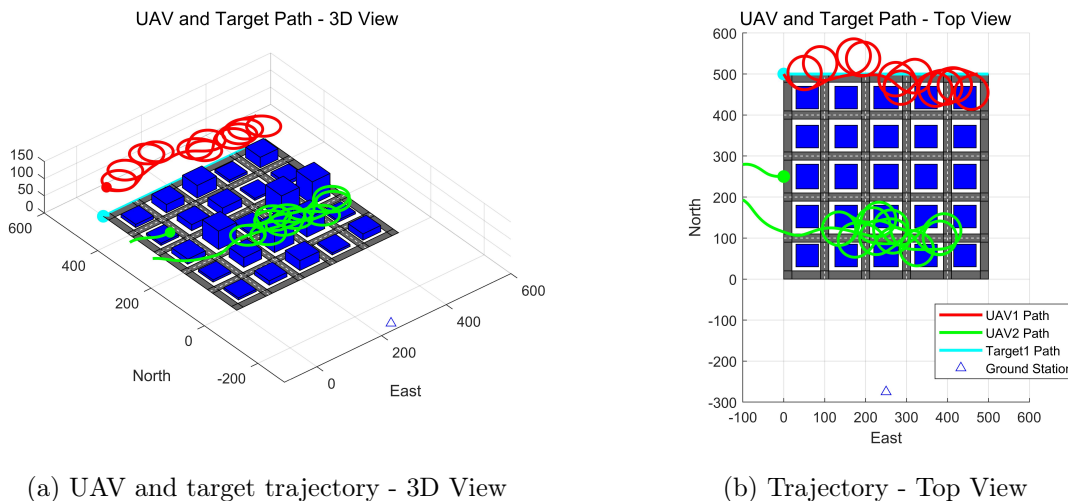(a) UAV and target trajectory - 3D View

(b) Trajectory - Top View

Figure 19: UAV and target trajectory with communication

Next case shows the simulation results when communication is considered in the same environment as Case 1 (See Figures 19 and 20). Figures 19a and 19b show the trajectory of each UAV. It can be seen as different from Case 1 because UAV 2 goes down and creates a trajectory
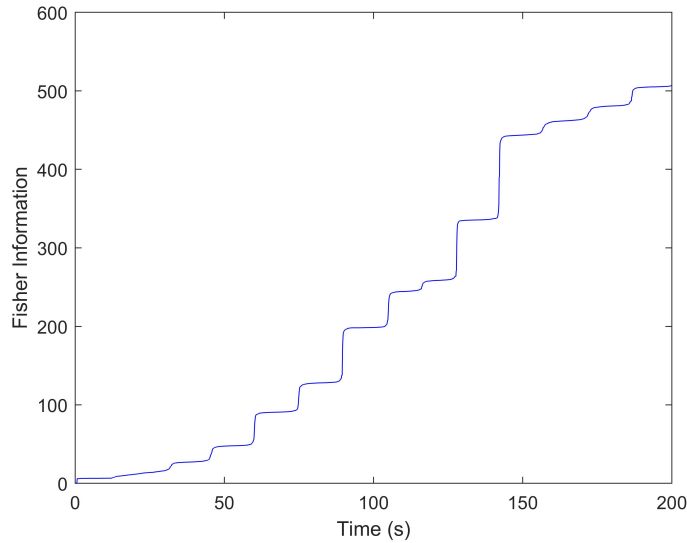
Figure 20: Trace of Fisher information at the ground station

acting as a relay by considering communication with the ground station using β. Therefore, it is possible to track the target while maintaining communication between UAVs and the ground station. Figures 20 shows the cumulated sum of trace of the Fisher information of the ground station over every time step. Unlike Case 1, since communication with the ground station is maintained continuously, the ground station can receive information about the target.

The third case performs MATLAB numerical simulation in 70 different environments to verify that the goal of this paper which is "find the UAVs' path and gimbal command to track the multiple targets in urban environments with maintaining communication to the ground station". Basically, a scenario is tracking nine targets in an urban environment using five UAVs. Also, to check whether communication with the ground station is appropriately considered, the target is initialized at a location far from the ground station. Again, it is assumed that the initial location of the target is known and the uncertainty is high.

This case is divided into two parts. First, in order to confirm the process of the proposed algorithm, one of the 70 simulations will be divided by a major timeline and explained. And secondly, we will analyze the performance of the proposed algorithm through the results of 70 simulations.

Figure 21-23 show the process of one of the 70 simulation results. The situation at 0, 12, and 30 seconds and the generated path will be discussed. Each figure consists of two parts. The figure on the left shows the current location of UAVs and targets. Cyan triangles represent UAV, and dots of various colors represent the targets. Each color means the cluster in which the target is contained. A blue triangle indicates the ground station, and its location is fixed outside the city. The figure on the right shows the estimation of UAV 1. Like the picture on the left, UAVs are represented by cyan triangles. In the case of targets, the blue circle represents the true position of the target, and the green circle represents the estimated target position.
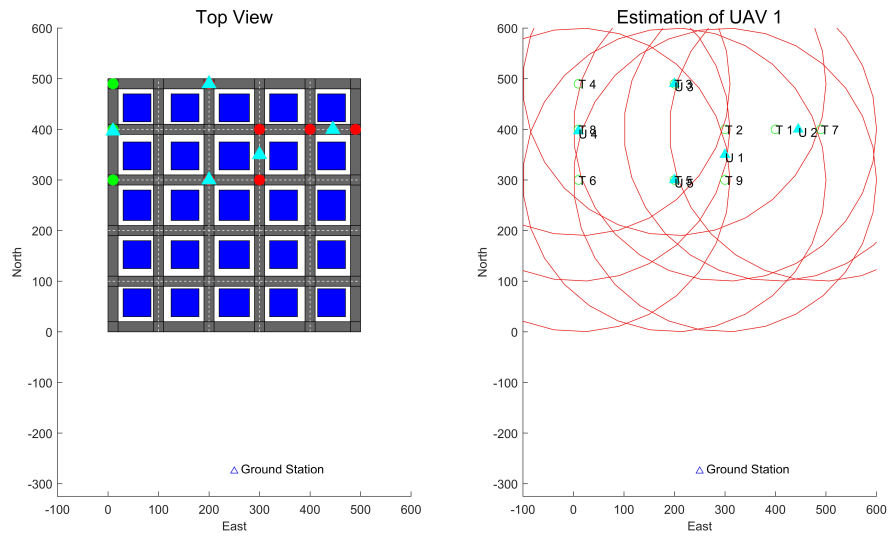
35

Figure 21: Simulation process at 0 sec

Also, the red ellipse around the estimated target position indicates the uncertainty of the target. As explained above, it was assumed that the initial position of the targets is known, and the uncertainty of estimate is high. Figure 21 shows the initial states of the simulation. Since the uncertainty of targets is high, the path to get as close to the target as possible is formed by J_2
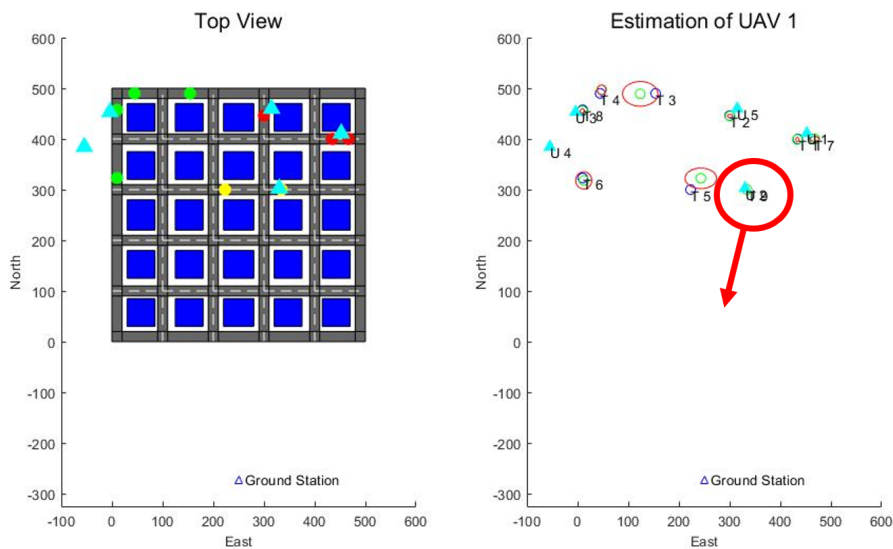

Figure 22: Simulation process at 12 sec

If the UAV follows the generated input for about 10 seconds, it can be seen that the overall target's uncertainty decreases, as shown in Figure 21. Thus, a trajectory that considers both communication and sensing is formed. At this time, UAV 2 in the red circle is going down in

36

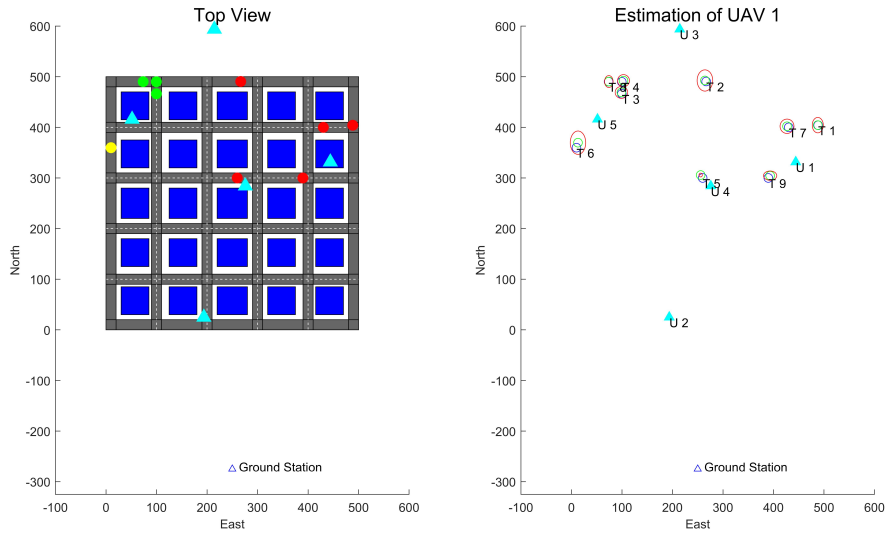the direction of the arrow to act as a communication relay.

Figure 23: Simulation process at 30 sec

Figure 21 shows the simulation result at 30 seconds. As illustrated in Figure 20, a trajectory for UAV 2 to approach and fly around the ground station is established. It can also be seen that the uncertainty about the target continues to remain low. In this way, it is confirmed that UAV 2 continuously acts as a relay or, depending on the situation, another UAV also acts as a relay while maintaining communication with the ground station and tracking targets continuously.
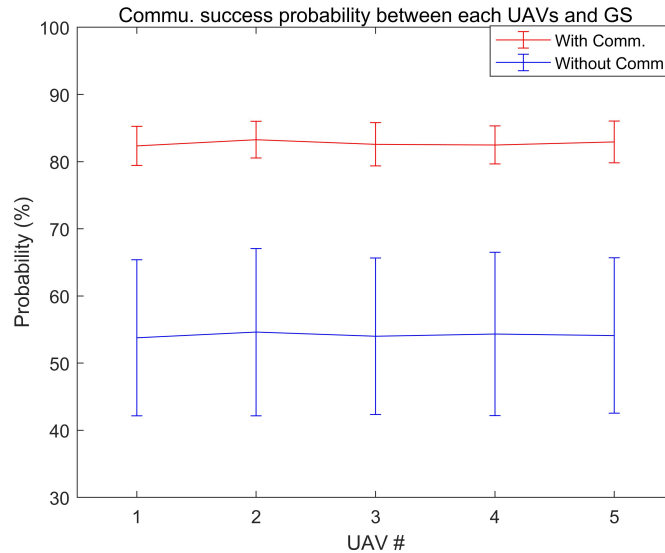

Figure 24: Average communication probability between the ground station and each UAVs

Finally, the results of 70 simulations are shown. Figure 24 shows the average probability of successful communication from each UAV to the ground station. The red line and blue line are the results of considering and not considering communication, respectively. If communication is
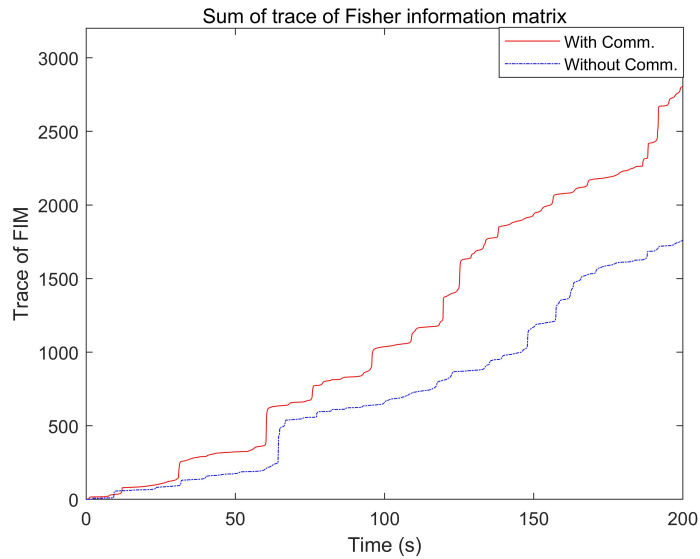
Figure 25: Trace of Fisher information at the ground station

not considered, the UAV's trajectory is dependent on the target's path, so on average, it has a communication success rate of 55% and a standard deviation of about 15%. However, if communication with the ground station is considered through the proposed algorithm, communication with the ground station is maintained by UAV acting as a communication relay, as shown in Figures 21-23. This can also be seen in Figure 24. As shown in Figure 24, it can be seen that there is an average performance improvement of about 30% in the red graph compared to the blue graph and the standard deviation is also greatly reduced.

As the overall communication performance improved, the estimation result at the ground station also improved. This can be seen in Figure 25. This figure shows the results of one of 70 simulations. Since the simulation was conducted in 70 random environments, the amount of information that can be theoretically obtained is different for each environment. Therefore, in this paper, one of the simulation results is shown as an example, and it is confirmed that Fisher information tends to be higher when communication is considered in other environments. The red and blue lines represent the cumulated sum of trace of Fisher information of every target when communication is considered and not considered, respectively. Here, traces of Fisher information for each target are obtained and compared using the summation of the trace. When communication is not considered, total Fisher information is low because there are many packet lost during communication with the ground station.

VI Conclusion and Future work

This paper proposes a cooperative multi target tracking algorithm that uses multiple UAVs while considering communication with ground stations in an urban environment. The proposed algorithm generates not only the trajectory of UAV but also the gimbal direction command. In addition, this method solved the problem of the previous work, planning the input when there is no predicted information in the prediction process of the receding horizon.

Numerical simulation through MATLAB environment is carried out in various initial conditions to verify the performance of the proposed algorithm. As a result, the mission success rate was improved by 30~40%, and the average successful transmission probability and the standard deviation is improved by 30% and 10%, respectively, compared to the previous work.

Future work is to test a broad map or more agile targets. Also, since the target motion model is too simple, there was a problem that the estimation error is increased in the intersection. To solve this, a constrained Kalman filter or IMM will be applied. In addition, to secure real-time performance, research is also needed to reduce computation time through model simplification used inside the receding horizon controller. Finally, after solving these problems, we will also proceed with flight tests.

References

[1] K. Kanistras, G. Martins, M. J. Rutherford, and K. P. Valavanis, "A survey of unmanned aerial vehicles (uavs) for traffic monitoring," in *2013 International Conference on Unmanned Aircraft Systems (ICUAS)*, 2013, pp. 221–234.

[2] T. Furukawa, F. Bourgault, B. Lavis, and H. F. Durrant-Whyte, "Recursive bayesian search-and-tracking using coordinated uavs for lost targets," in *Proceedings 2006 IEEE International Conference on Robotics and Automation, 2006. ICRA 2006.*, 2006, pp. 2521–2526.

[3] P. Yao, W. Honglun, and H. Ji, "Gaussian mixture model and receding horizon control for multiple uav search in complex environment," *Nonlinear Dynamics*, vol. 88, 04 2017.

[4] S. Papaioannou, P. Kolios, T. Theocharides, C. G. Panayiotou, and M. M. Polycarpou, "Probabilistic search and track with multiple mobile agents," in *2019 International Conference on Unmanned Aircraft Systems (ICUAS)*, 2019, pp. 253–262.

[5] S. Zhu and D. Wang, "Ground target tracking using uav with input constraints," *Journal of Intelligent and Robotic Systems*, vol. 65, pp. 521–532, 01 2012.

[6] S. Park, "Circling over a target with relative side bearing," *Journal of Guidance, Control, and Dynamics*, vol. 39, no. 6, pp. 1454–1458, 2016. [Online]. Available: https://doi.org/10.2514/1.G001421

[7] Zhijun Tang and U. Ozguner, "Motion planning for multitarget surveillance with mobile sensor agents," *IEEE Transactions on Robotics*, vol. 21, no. 5, pp. 898–908, 2005.

[8] S. Ponda, R. Kolacinski, and E. Frazzoli, "Trajectory optimization for target localization using small unmanned aerial vehicles," *AIAA Guidance, Navigation, and Control Conference*, 2009.

[9] S. Park, "Guidance law for standoff tracking of a moving object," *Journal of Guidance, Control, and Dynamics*, vol. 40, no. 11, pp. 2948–2955, 2017. [Online]. Available: https://doi.org/10.2514/1.G002707

[10] H. Oh, S. Kim, H. Shin, and A. Tsourdos, "Coordinated standoff tracking of moving target groups using multiple uavs," *IEEE Transactions on Aerospace and Electronic Systems*, vol. 51, no. 2, pp. 1501–1514, 2015.

[11] E. W. Frew, D. A. Lawrence, and S. Morris, "Coordinated standoff tracking of moving targets using lyapunov guidance vector fields," *Journal of Guidance, Control, and Dynamics*, vol. 31, no. 2, pp. 290–306, 2008. [Online]. Available: https://doi.org/10.2514/1.30507

[12] N. Farmani, L. Sun, and D. Pack, "An optimal sensor management technique for unmanned aerial vehicles tracking multiple mobile ground targets," in *2014 International Conference on Unmanned Aircraft Systems (ICUAS)*, 2014, pp. 570–576.

[13] ——, "Tracking multiple mobile targets using cooperative unmanned aerial vehicles," in *2015 International Conference on Unmanned Aircraft Systems (ICUAS)*, 2015, pp. 395–400.

[14] J. H. Taylor, "The cramer-rao estimation error lower bound computation for deterministic nonlinear systems," in *1978 IEEE Conference on Decision and Control including the 17th Symposium on Adaptive Processes*, 1978, pp. 1178–1181.

[15] H. Oh, S. Kim, H. Shin, and A. Tsourdos, "Coordinated standoff tracking of moving target groups using multiple uavs," *IEEE Transactions on Aerospace and Electronic Systems*, vol. 51, no. 2, pp. 1501–1514, 2015.

[16] J. Manyika and H. Durrant-Whyte, *Data Fusion and Sensor Management: A Decentralized Information-Theoretic Approach.* USA: Prentice Hall PTR, 1995.

[17] M. Ridley, E. Nettleton, A. Göktogan, G. Brooker, S. Sukkarieh, and H. F. Durrant-Whyte, "Decentralised ground target tracking with heterogeneous sensing nodes on multiple uavs," in *Information Processing in Sensor Networks*, F. Zhao and L. Guibas, Eds. Berlin, Heidelberg: Springer Berlin Heidelberg, 2003, pp. 545–565.

[18] D. W. Casbeer and R. Beard, "Distributed information filtering using consensus filters," in *2009 American Control Conference*, 2009, pp. 1882–1887.

[19] Y. S. Kim, J. H. Lee, H. M. Do, B. K. Kim, T. Tanikawa, K. Ohba, G. Lee, and S. H. Yun, "Unscented information filtering method for reducing multiple sensor registration error," in *2008 IEEE International Conference on Multisensor Fusion and Integration for Intelligent Systems*, 2008, pp. 326–331.

[20] P. Yang, R. A. Freeman, and K. M. Lynch, "Distributed cooperative active sensing using consensus filters," in *Proceedings 2007 IEEE International Conference on Robotics and Automation*, 2007, pp. 405–410.

[21] T. H. Chung, J. W. Burdick, and R. M. Murray, "A decentralized motion coordination strategy for dynamic target tracking," in *Proceedings 2006 IEEE International Conference on Robotics and Automation, 2006. ICRA 2006.*, 2006, pp. 2416–2422.

[22] B. Schlotfeldt, D. Thakur, N. Atanasov, V. Kumar, and G. J. Pappas, "Anytime planning for decentralized multirobot active information gathering," *IEEE Robotics and Automation Letters*, vol. 3, no. 2, pp. 1025–1032, 2018.

[23] D. Shin, Y. Song, J. Oh, and H. Oh, "Nonlinear disturbance observer-based standoff target tracking for small fixed-wing uavs," *International Journal of Aeronautical and Space Sciences*, 04 2020.

[24] H. Chen, K. Chang, and C. S. Agate, "Uav path planning with tangent-plus-lyapunov vector field guidance and obstacle avoidance," *IEEE Transactions on Aerospace and Electronic Systems*, vol. 49, no. 2, pp. 840–856, 2013.

[25] S. Lim, Y. Kim, D. Lee, and H. Bang, "Standoff target tracking using a vector field for multiple unmanned aircrafts," *Journal of Intelligent and Robotic Systems*, vol. 69, 01 2013.

[26] S. Park and D. Jung, "Vision-based tracking of a ground-moving target with uav," *International Journal of Aeronautical and Space Sciences*, vol. 20, 01 2019.

[27] P. Yao, H. Wang, and H. Ji, "Multi-uavs tracking target in urban environment by model predictive control and improved grey wolf optimizer," *Aerospace Science and Technology*, vol. 55, pp. 131 – 143, 2016. [Online]. Available: http://www.sciencedirect.com/science/article/pii/S1270963816301869

[28] R. Sharma, "Cooperative sensor resource management for multi target geolocalization using small fixed-wing unmanned aerial vehicles," 08 2013.

[29] N. Farmani, L. Sun, and D. J. Pack, "A scalable multitarget tracking system for cooperative unmanned aerial vehicles," *IEEE Transactions on Aerospace and Electronic Systems*, vol. 53, no. 4, pp. 1947–1961, 2017.

[30] P. Skoglar, U. Orguner, D. Törnqvist, and F. Gustafsson, "Road target search and tracking with gimballed vision sensor on an unmanned aerial vehicle," *Remote Sensing, vol. 4, issue 7, pp. 2076-2111*, vol. 4, pp. 2076–2111, 07 2012.

[31] Z. Liu, X. Fu, and X. Gao, "Co-optimization of communication and sensing for multiple unmanned aerial vehicles in cooperative target tracking," *Applied Sciences*, vol. 8, p. 899, 05 2018.

[32] R. W. Beard and T. W. McLain, *Small Unmanned Aircraft: Theory and Practice*. USA: Princeton University Press, 2012.

Acknowledgements

I finished my two years of master's course and submitted my thesis. There are many people who have helped me over the past two years. I am still not good enough, but I would like to express my gratitude to them as I finish my degree.

I sincerely thank Professor Hyondong Oh, who helped me the most and guide my shortcomings carefully. When I lost my confidence and wanted to give up my studies, I would not have been able to submit this thesis without Prof. Hyondong Oh's advice and encouragement. I would also like to thank those who worked with me in the autonomous systems laboratory. I learned a lot from them and I was able to have fun even though master's course was hard.

Lastly, I would like to thank my family for supporting me up to my master's degree. I would not have completed this degree if they had not believed in me and encouraged me even though I entered graduate school at a considerable age.

Thank you.